AFRL-DE-TR-
2001-1090

FIBER LASER ARRAY

Thomas B. Simpson

Jaycor, Inc.
3394 Carmel Mountain Road
San Diego, CA 92121

January 2002

Final Report

APPROVED FOR PUBLIC RELEASE; DISTRIBUTION IS UNLIMITED.

AIR FORCE RESEARCH LABORATORY
Directed Energy Directorate
3550 Aberdeen Ave SE
AIR FORCE MATERIEL COMMAND
KIRTLAND AIR FORCE BASE, NM 87117-5776

20020717 160

AFRL-DE-TR-2001-1090

Using Government drawings, specifications, or other data included in this document for any purpose other than Government procurement does not in any way obligate the U.S. Government. The fact that the Government formulated or supplied the drawings, specifications, or other data, does not license the holder or any other person or corporation; or convey any rights or permission to manufacture, use, or sell any patented invention that may relate to them.

This report has been reviewed by the Public Affairs Office and is releasable to the National Technical Information Service (NTIS). At NTIS, it will be available to the general public, including foreign nationals.

If you change your address, wish to be removed from this mailing list, or your organization no longer employs the addressee, please notify AFRL/DELO, 3550 Aberdeen Ave SE, Kirtland AFB, NM 87117-5776.

Do not return copies of this report unless contractual obligations or notice on a specific document requires its return.

This report has been approved for publication.

Dr. Phillip Peterson

DR. PHILLIP PETERSON
Project Manager

FOR THE COMMANDER

LeAnn S. Brasure

LE ANN BRASURE, Lt Col, USAF
Chief, High Power Solid-State
Laser Branch

R. Earl Good

R. EARL GOOD, SES
Director, Directed Energy Directorate

REPORT DOCUMENTATION PAGE

Form Approved
OMB No. 0704-0188

Public reporting burden for this collection of information is estimated to average 1 hour per response, including the time for reviewing instructions, searching existing data sources, gathering and maintaining the data needed, and completing and reviewing this collection of information. Send comments regarding this burden estimate or any other aspect of this collection of information, including suggestions for reducing this burden to Department of Defense, Washington Headquarters Services, Directorate for Information Operations and Reports (0704-0188), 1215 Jefferson Davis Highway, Suite 1204, Arlington, VA 22202-4302. Respondents should be aware that notwithstanding any other provision of law, no person shall be subject to any penalty for failing to comply with a collection of information if it does not display a currently valid OMB control number. **PLEASE DO NOT RETURN YOUR FORM TO THE ABOVE ADDRESS.**

1. REPORT DATE (DD-MM-YYYY)	2. REPORT TYPE	3. DATES COVERED (From - To)
08-01-2002	Final Technical Report	November 1999- November 2001

4. TITLE AND SUBTITLE
Fiber Laser Array

5a. CONTRACT NUMBER
F29601-00-C-0001

5b. GRANT NUMBER

5c. PROGRAM ELEMENT NUMBER
62605F

6. AUTHOR(S)
Thomas B. Simpson

5d. PROJECT NUMBER
4866

5e. TASK NUMBER
LR

5f. WORK UNIT NUMBER
02

7. PERFORMING ORGANIZATION NAME(S) AND ADDRESS(ES)

Jaycor, Inc.
3394 Carmel Mountain Road
San Diego, CA 92121

8. PERFORMING ORGANIZATION REPORT NUMBER
D01-252

9. SPONSORING / MONITORING AGENCY NAME(S) AND ADDRESS(ES)
AFRL/DELO
3550 Aberdeen Avenue SE
Kirtland AFB, NM 87117-5776

10. SPONSOR/MONITOR'S ACRONYM(S)

11. SPONSOR/MONITOR'S REPORT NUMBER(S)
AFRL-DE-TR-2001-1090

12. DISTRIBUTION / AVAILABILITY STATEMENT

Approved for public release; distribution unlimited.

13. SUPPLEMENTARY NOTES
The views, opinions and/or findings contained in this report are those of the author(s) and should not be construed as an official Department of the Air Force position, policy or decision, unless so designated by other documentation.

14. ABSTRACT

Investigations of the coherent combining of fiber lasers using intracavity coupling have focused on the use of the Talbot effect, an external master oscillator, and the use of coherent coupling to create nonlinear, i.e. field-dependent, loss within the coupled laser array. During this program, Jaycor focused on the construction and use of an experimental apparatus that can be used to investigate the coherent combination of an array of fiber lasers. The apparatus was designed to emphasize reconfiguration flexibility and permit a wide range of key parameters to be varied. These include key laser cavity parameters, such as gain and output coupling, and key array parameters, such as the amplitude and phase of mutually coupled fields. Coherent intracavity coupling of large arrays is complicated by the presence of multiple longitudinal modes that can be simultaneously supported by the individual lasers. These individual modes do not, in general, have the same optical frequencies as one moves across the elements. While two element arrays can be easily operated in a coherent fashion, four element arrays showed a lower fraction of coherent power and greater sensitivity to fluctuations of the laboratory environment.

15. SUBJECT TERMS
Coherent Coupling of Lasers — Erbium-doped Fiber Amplifier — Fiber Laser
Injection Locking — Laser Array — Nonlinear Dynamics

16. SECURITY CLASSIFICATION OF:			17. LIMITATION OF ABSTRACT	18. NUMBER OF PAGES	19a. NAME OF RESPONSIBLE PERSON
a. REPORT	b. ABSTRACT	c. THIS PAGE			Dr. Phillip Peterson
Unclassified	Unclassified	Unclassified	Unlimited	56	19b. TELEPHONE NUMBER (include area code) 505-846-9301

Standard Form 298 (Rev. 8-98)
Prescribed by ANSI Std. 239.18

CONTENTS

LIST OF FIGURES

ACKNOWLEDGEMENTS

The work and results described here have been undertaken with the ongoing collaboration of Drs. Phillip Peterson and Athanaseos Gavrielides of the Air Force Research Laboratory. The author is indebted to them for their encouragement, support and willingness to dig into the details of this problem and search for the answers. Their parallel theoretical investigations have helped provide an underpinning for the picture of the interactions that induce the key phenomena described here. Also, the author gratefully acknowledges expert technical assistance with the experimental apparatus by Mr. Frank Doft.

SUMMARY

A flexible, reconfigurable experimental apparatus has been designed and configured to investigate the coherent combining of fiber lasers through intracavity coupling. The design has emphasized the use of commercially available components being developed for the telecommunications industry. The apparatus is built around four independent Erbium-doped fiber amplifiers, configured with fiber Bragg gratings as high reflectors, and intracavity coupling schemes based on either 2×2, 50/50 fiber couplers with a common output coupler, or the self-imaging (Talbot) effect. Polarization control for the intracavity fields is also provided.

Measurements taken with this apparatus using the 2×2 fiber-coupler configuration show that intracavity-coupled lasers will spontaneously adjust their optical output to achieve a coherently combined output. With a two-laser array, the coherent coupling is robust, and over 90% of the optical output is coherently coupled from the laser cavity through the common output coupler. A four-element array showed a lower fraction of coherent coupling, typically around 75%, and its output was much more sensitive to fluctuations of the laboratory environment. In either case, the polarization of the laser fields had to be adjusted to obtain maximum coherent coupling.

Optical spectra and power spectra of the photodetector signal of the array output show that the solitary laser consists of a sparse set of optical modes with significant optical power, typically 10-20 out of 10^4 available modes within the high-reflection band of the fiber Bragg grating. Similar optical spectra were obtained under coherent intracavity coupling, except that isolated modes could become mode clusters. The optical frequencies of the cavity modes varied from laser to laser across the array due to variations in cavity length. When coupled, the mode frequencies were pulled away from the isolated mode frequencies showing that the coherent coupling proceeded on a mode to mode basis.

The need for mode to mode coherent coupling explains the observation of increasing difficulty in coherently combined output as the number of lasers is increased. It becomes increasingly difficult to find modes with good frequency overlap across the array. Therefore, cavity length or phase control may be required if intracavity coupling is to be used to try to coherently couple an array consisting of many elements.

INTRODUCTION

Recent advances in fiber lasers pumped by laser diodes have shown that this system can deliver high continuous output power from a rugged, all solid-state system. Output powers in excess of 100 Watts (W) have been reported from individual fiber lasers [1], with commercially available units delivering over 40 W. Recent analytical work has suggested that powers up to the kilowatt (kW) level might be possible from individual fiber lasers [2]. Achieving considerably higher power in a coherent beam will require the coherent combining of the output from several fiber lasers or amplifiers. Such high powers may be needed for coherent scene illumination for imaging and laser-radar applications, particularly for space-based systems. A variety of techniques can be used to generate coherent beams from multiple sources. These include mutual coupling of the sources to lock them together, and locking the sources to a single master laser. The mutual coupling can be done through mutual injection of the beams within a single cavity. The Talbot effect, or the self-imaging properties of periodic optical structures, has been used to coherently combine the output from laser diode arrays. Coupling through injection by a master oscillator can be achieved in either optical cavity or optical amplifier configurations where there is a means to control the optical path length.

In this program, we have investigated the coherent combining of fiber lasers using intracavity coupling. While originally focused on the use of the Talbot effect and/or an external master oscillator, the investigations have broadened to address the use of coherent coupling to create field-dependent loss within the coupled laser array. The potential importance of this mechanism to the intracavity coherent coupling of fiber lasers was not recognized when this program was initiated. During the program, the focus of the work at Jaycor has been on the construction and use of a flexible experimental apparatus to investigate the coherent combination of an array of fiber lasers. The apparatus has been designed to emphasize reconfiguration flexibility and permit a wide range of key parameters to be varied. These include key laser cavity parameters, such as gain and output coupling, key array parameters, such as the amplitude and phase of mutually coupled fields, and key external influences, such as injected optical signals. The apparatus was designed to investigate the use of the self-imaging properties of periodic optical structures, the

Talbot effect, for generation of coherent output. Additionally, injection locking using an external optical source was implemented.

This final report describes the results of the investigations. Following this introduction, we describe the flexible experimental apparatus that has been constructed to study coherent intracavity coupling in fiber lasers. This is followed by a description of the output characteristics of an individual array element when subjected to external optical injection, or to feedback from a fiber Bragg grating (FBG). We then continue with key experimental results for a two-element configuration and the results of measurements of the full four-element array. Our key conclusion is that coherent intracavity coupling of large arrays is complicated by the presence of multiple longitudinal modes that can be simultaneously supported by the individual lasers. These individual modes do not, in general, have the same optical frequencies in the individual array elements. This is due to the fact that it is practically impossible to match the cavity lengths of the different laser elements of the array. While two element arrays can be easily operated in a coherent fashion, four-element arrays showed a lower fraction of coherent power and greater sensitivity to fluctuations of the laboratory environment. We conclude by suggesting further work that might overcome the observed limitations.

FIBER ARRAY EXPERIMENTAL APPARATUS

The experimental apparatus was constructed with attention to two key goals. First, it was to be flexible to allow a variety of cavity implementations to be configured and easily reconfigured. Second, to the greatest extent possible, it was built using commercially available components to minimize cost and maximize flexibility, ease of use, and the ability to incorporate design changes as the program progressed. Throughout, the apparatus design emphasized the use of cost-effective, commercially available fiber components being developed for the telecommunications industry. The array is designed around Erbium (Er)-doped fibers as the amplifying medium. Er-doped fiber amplifiers are now available from a variety of vendors. Most units, however, are focused on the telecommunications market and do not emphasize high powers. Because high power applications are of significant interest to the Air Force, we were interested in fiber gain media that could be scaled to high power levels. Dual-cladding or cladding-pumped fibers have been used almost exclusively in the fiber laser systems that have achieved the highest power levels. Therefore, we were interested in using these fibers as the gain media for the array. Following discussions with IPG Photonics, US distributor for IRE Polus Group, we were able to order a four-element, Er-doped fiber amplifier array that incorporates the dual cladding fibers. Each element is under independent gain control and is individually connectorized for coupling to additional optical elements. There is no internal crosstalk between elements of the amplifier array so that all coupling is under external control. The use of connectorized optical fiber components allows ready reconfiguration of the array. All connectors for the array are of the FC/APC type. These connectors introduce very small loss, <0.5 dB, and minimal reflections, <60 dB, in the optical cavity. Minimizing unwanted reflections is essential for control of the coupling between the individual cavities of the fiber laser array.

The four-element, semi-custom array is actually only a slightly modified variant of standard catalog products, with the only difference being in the packaging of the amplifiers and the associated optical isolators. Two amplifiers each are packaged in a housing shown in Figure 1. Approximately one-meter fiber pigtails for each input and output extend from the housing. The fiber pigtails are made from industry-standard, single-mode SMF-28 equivalent fiber and are

terminated with FC/APC connectors. The fiber maintains the fundamental spatial mode for the 1.55 micrometer (μm) light but does not maintain polarization. The amplifiers are pumped by laser diodes internal to the packaging. Electrical power to the diodes is supplied through a connector with knobs that can be turned to adjust the pumping level. Electrical requirements are approximately 6.5- 9 volts dc at 1.5 amps per amplifier for full power operation. Power from the pump laser diodes can be modulated at multi-megahertz rates using a function generator and home-built connector.

Figure 1. Packaged unit containing two Er-doped fiber amplifiers capable of 40-dB small-signal gain and 100 mW saturated output power. The input and output fiber pigtails are visible on the right side. Electrical power to the laser diodes used to pump the fiber amplifiers comes through the connector above. For scale, the table holes are on one-inch centers

Associated with each amplifier was a separate package containing four optical isolators, shown in Figure 2. In a standard single-pass amplifier configuration there would be optical isolators on the input and output sides of the fiber amplifier. Because we are interested in producing a laser configuration, we had the isolators packaged separately. Both amplifiers and associated isolators are shown together in Figure 3.

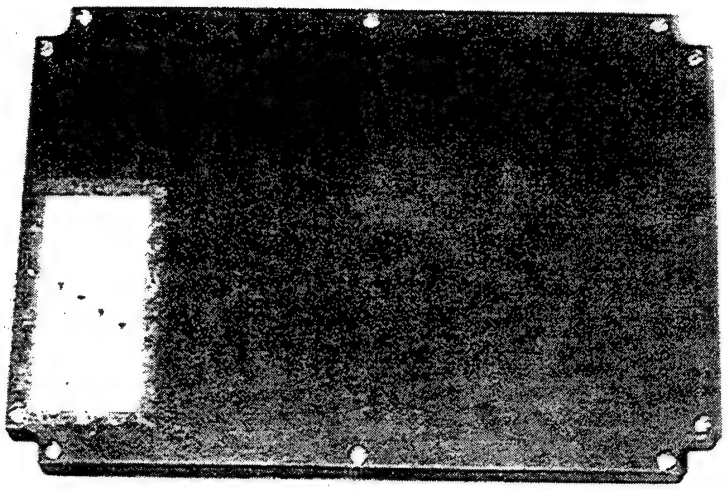

Figure 2. Packaged unit containing four optical isolators capable of >30 dB one way optical attenuation. The input and output fiber pigtails are visible on the right side. All are FC/APC connectorized.

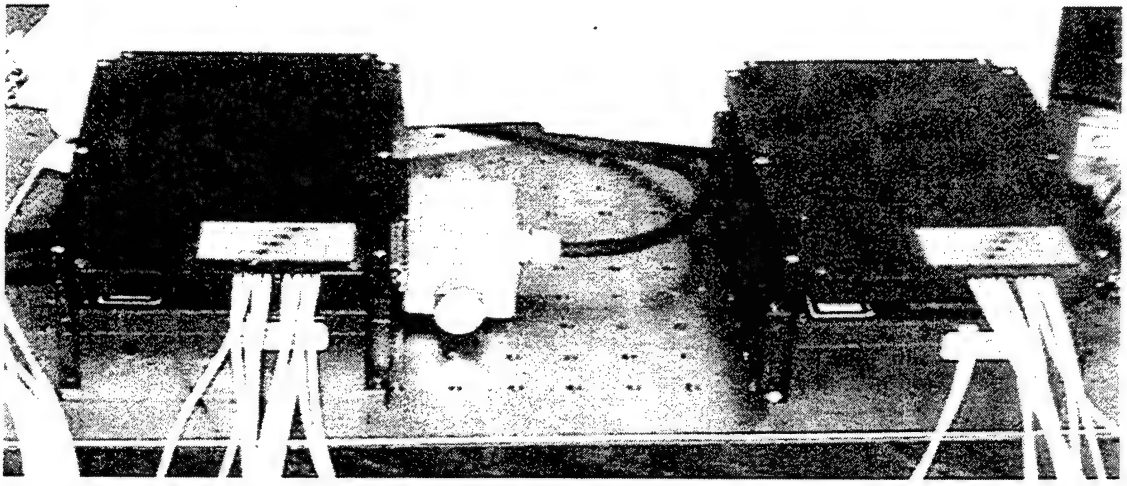

Figure 3. Optical isolator packages sitting on top of associated Er-doped fiber amplifier units. Fiber pigtails are coming out of the fronts of the units. Electrical control connector for one amplifier package is visible on right side. For scale, table holes are on one-inch centers.

Because the optical isolators have been separated from the Er-doped amplifiers laser light can propagate in both directions through the amplifiers. There is some asymmetry due to the way that the amplifiers are pumped by the laser diodes. More power is pumped into the "output" ends of the amplifiers than the "input" ends. However, the results presented in this report use relatively low circulating power levels in the lasers and this is not a significant factor.

In addition to the gain region each laser cavity in the array must contain a high reflector, an output coupler, and an intracavity coupling element. Additionally, we found it necessary to introduce polarization control to achieve coherent coupling. Intracavity coupling was achieved in two ways. One was an all-fiber configuration built around fiber couplers. The fiber couplers are symmetric four-port elements with each of two inputs equally coupled to two output ports. The apparatus is shown in Figure 4. The figure shows the configuration used for the full, four-element array. On the left are four polarization rotators, one for the laser field from each amplifier. The output from each polarizer is coupled into on port of the symmetric 50/50 couplers. A tree of three couplers is required to mutually couple all of the elements of the array. The

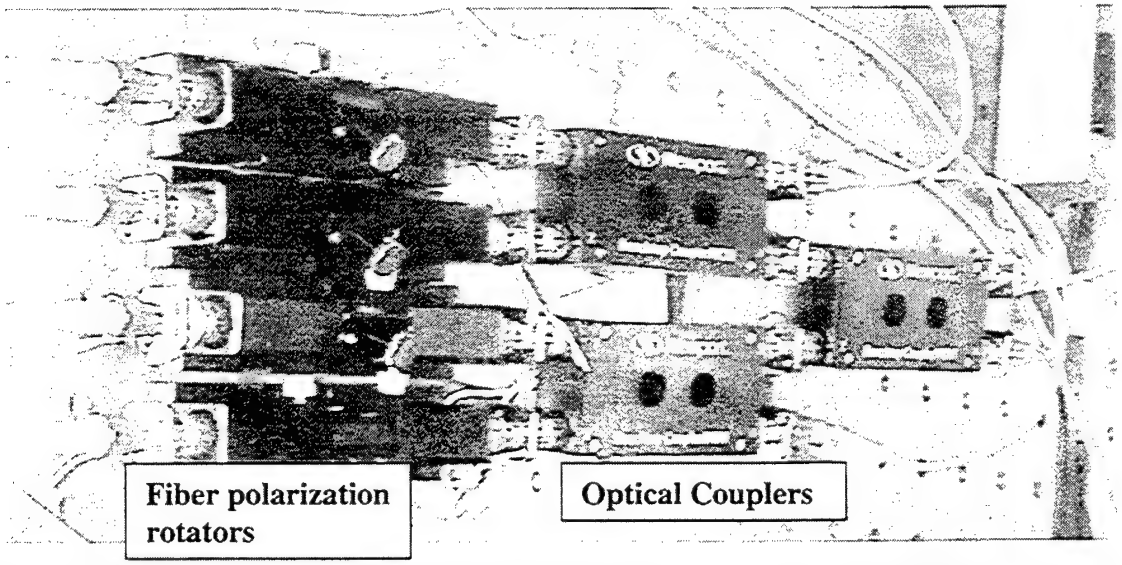

Figure 4. Coherent intracavity coupling apparatus for a four-element fiber-laser array consisting of four fiber polarization rotators and three symmetric 50/50 optical couplers.

polarizer/coupler combination is placed between the amplifier "output" and a common output coupler of the array. There are three unconnected, "loss" ports on the coupler tree. The inputs from the four Er-doped fiber amplifiers are shown on the left and the output to the common output coupler is on the top right. There are also three loss ports connected to optical isolators. The common output coupler used for most of the measurements was an uncoated fiber collimator. The flat surface of the fiber collimator provided approximately 4% reflection back into the optical cavity. Light coupled out from the collimator could be passed through a polarizing beamsplitter cube and the resolved polarizations collected by subsequent fiber collimators and routed to photodetectors. This apparatus is shown in Figure 5.

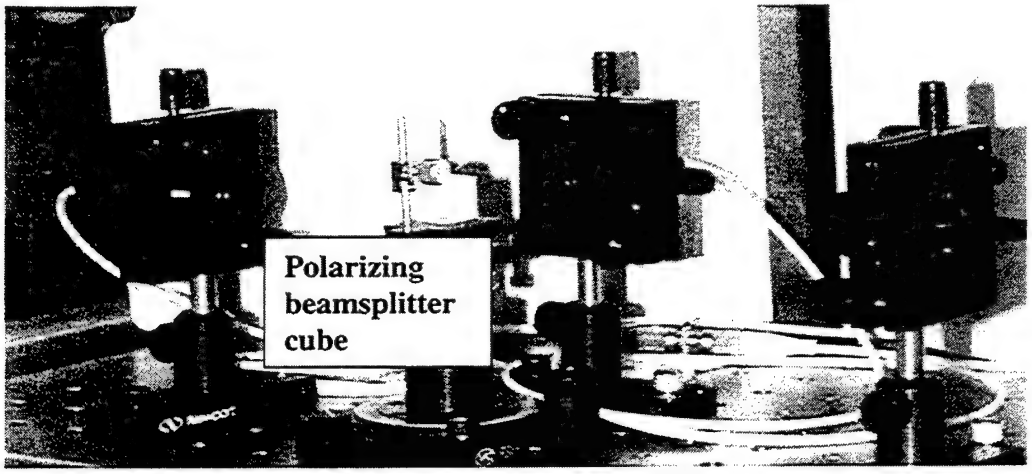

Figure 5. Output apparatus of the all-fiber intracavity coupling configuration. The fiber collimator used as the output coupler is in the optical mount of the right. A polarizing beamsplitter separates orthogonal polarizations and the polarized array output is collected into fiber collimators in the other optical mounts to be routed to photodetectors.

The second intracavity-coupling configuration used a free-space field-coupling region to implement the mutual coupling. This intracavity-coupling region contained the requisite characteristics for the Talbot Effect, or array self-imaging, to be displayed. Our design called for the region of array self-imaging at the output coupler end of the cavity. This insured that the coherence would be achieved at the laser output. A key reason for this is that it is unlikely that we could maintain sub-micron precision on the length of the different fiber laser cavities in the

array. Therefore, if we placed the self-imaging region at the high-reflector end of the laser cavity, the coherence would be essentially randomized at the output coupler end. At the output coupler end, the output from the individual fiber amplifiers is launched into free space using a fiber array or fiber collimator array built using silicon V-groove technology. We identified two linear arrays from ACT Micro Devices, one consisting of anti-reflection (AR) coated fibers and the other consisting of fiber-coupled gradient index (GRIN) lenses, both with 250 μm periods. The smaller diffraction from the GRIN lens collimators means that coupling between nearest neighbors will be relatively much stronger. The fiber array is a standard product consisting of sixteen elements and the collimator array is a now-discontinued standard product consisting of eight elements. Extra elements, relative to the amplifier array, were included in the V-groove arrays to allow for damage of individual elements and to allow for the counter-propagating fields within the laser arrays to be coupled into different elements of the Talbot array, if desired. A cylindrical lens and 95 % reflecting optical flat completed the self-imaging cavity with the collimator array configuration. This is shown in Figure 6. The 250 μm spacing between elements in the arrays corresponds to a Talbot, or self-imaging, distance of approximately 8 cm for the 1.55 μm output from the Er-doped fiber lasers.

The optical cavities use fiber Bragg gratings (FBGs) as the high reflector. Using gratings designed for the ITU grid defined for wavelength division multiplexed (WDM) optical communication systems, we are able to take advantage of low-cost, commercially available components. FBGs with a wide range of reflectances are available for the wavelength region covered by Er-doped fiber amplifiers. Initially we identified Thorlabs as the best source. During the program, they dropped their low-cost FBGs and we purchased additional gratings from BTI Photonics at a similar cost. Thorlabs could not perform the connectorization of these elements to FC/APC connectors and maintain reasonable length uniformity so that Rifocs Corporation performed the connectorization of the fibers. The pigtails were kept the same length for uniformity across the array. The FBGs are pictured in Figure 7. Their maximum reflectivity is centered around 1.557 μm, and the frequency width is approximately 100 GHz to match the ITU grid.

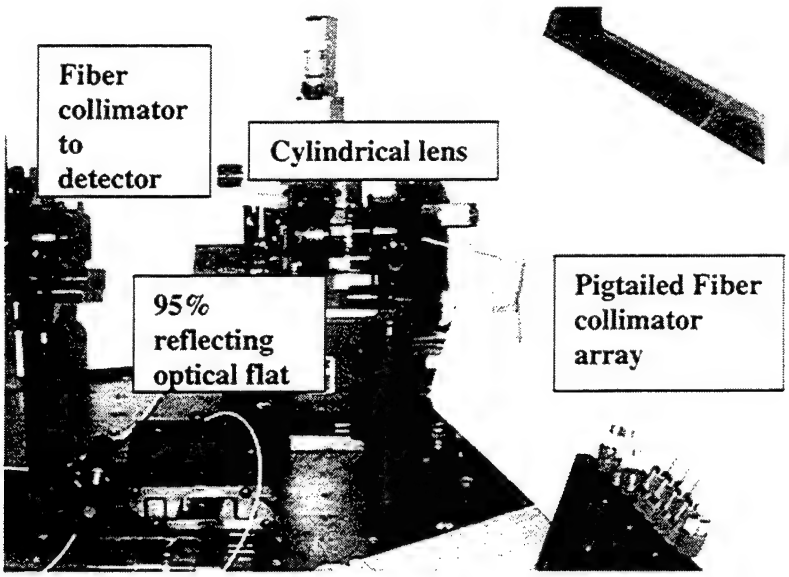

Figure 6. Apparatus for Talbot cavity implementation of the intracavity coherent coupling. The intracavity laser fields are launched from the pigtailed fiber collimator array into free space. The pas through a cylindrical lens before reaching the array output coupler, a 95% reflecting optical flat. The laser field transmitted through the flat is collected by a fiber collimator before being passed to a photodetector.

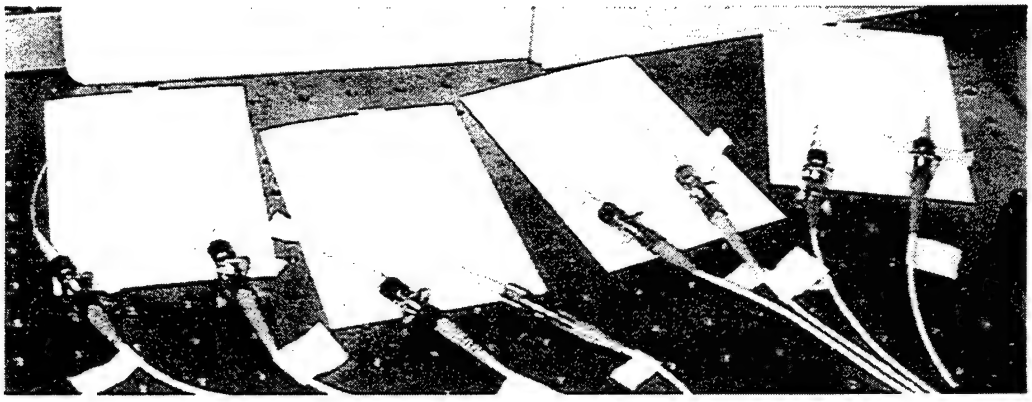

Figure 7. Picture of four FBGs with connectorized pigtails for the four-element array.

A key uniformity specification relates to the optical path length of the individual elements of the array. For each component, the length uniformity could be specified to no better than ± 1 cm. Therefore, cavity length variations on the order of or greater than 1 cm will be present in the fiber laser array. Such variations will between 0.1-1% of the total cavity length. Because of the coherent nature of the intracavity coupling, this had a significant effect on performance.

The design for the experimental apparatus also included provision for external optical injection from a low-noise, master laser. Here again, the use of the Er-doped fiber gain medium allowed extensive use of coupling via the fiber components developed for the telecommunications industry. Packaged distributed feedback (DFB) semiconductor laser diodes with operating wavelengths that can be specified across the ITU grid are available from a variety of vendors. In independent tests underway in our laboratory, we confirmed that the spurious reflections from the more common and less expensive FC/PC connectors were likely to cause serious problems with the operation of a laser array. We observed that back reflections from an FC/PC connector were sufficient to induce the state of coherence collapse in a semiconductor laser. While individual fiber lasers are not expected to have the same sensitivity to unwanted feedback as individual semiconductor lasers, a fiber array based on intracavity coupling may be quite sensitive. Therefore, the choice of FC/APC connectors in our reconfigurable design appears to be fully warranted. It should be clarified that as the system is scaled to high powers all intracavity connectors will have to be replaced by fiber splicing techniques. The heating due to losses and imperfections at the connectors would otherwise lead to catastrophic damage. However, by using the standard fiber connectors we will be able to readily reconfigure the array to investigate new phenomena.

We also used external optical injection from a distributed feedback laser diode that operates within the high reflectivity window of the Bragg gratings to aid in the testing of the array components and in the alignment of the components for coherent coupling. The use of a coherent external optical source allows comparison of the field generated internally through amplification and feedback of spontaneous emission with an externally coupled field of known properties and good coherence. In addition, it was postulated that a combination of external optical injection and array self-imaging might produce a better overall output from the array than can be achieved with either technique alone. However, as we show below, this was not found to be true in our configuration.

The optical characteristics of the array, and its individual components, were monitored using a variety of photodiodes that were coupled to the various output ports of the configuration. Details

of the experimental configurations for the various tests will be given in following sections. Included among the photodiodes was one that had a bandwidth of greater than 10 GHz. Using this in combination with a microwave spectrum analyzer made the generation of broadband spectra possible. This detector also provided a signal proportional to the average output power that had a bandwidth of a few kHz. Temporal characteristics were monitored using various oscilloscopes.

Power spectra of the photodiode signal were also generated. The photodetector output was amplified with an 18 GHz-bandwidth microwave amplifier and this signal was directly fed to a microwave spectrum analyzer. Optical spectra were generated using a heterodyne technique with a distributed feedback (DFB) laser diode acting as the local oscillator. By ramping the bias current to the laser diode its optical frequency of the local oscillator could be swept over a range of approximately 25 GHz with a spectral resolution of approximately 100 MHz. Because the mode spacing of the fiber lasers is approximately 6 MHz, this resolution did not permit the isolation of individual modes in the optical spectrum. We found that the lasers operated on more than one mode simultaneously, so we could investigate the individual mode characteristics by monitoring the power spectrum of the photodetected signal.

CHARACTERIZATION OF ARRAY COMPONENTS

The output of the array depends on the characteristics of individual components. Apparatus used for testing of the Er-doped fiber amplifiers is shown schematically in Figure 8. Two configurations were set up. The first, Figure 8(a), tested the amplifier in its design configuration, while the second, Figure 8(b), used a fiber Bragg grating to produce feedback and, nominally, a two-pass amplifier configuration. After passing through an optical isolator, the output was passed from fiber to free space through one of the 16 elements of the V-groove fiber array. The array was positioned to be at the entrance slit point of a 0.125 meter Spex scanning monochrometer. A fiber collimator was placed beyond the output slit to collect the output signal and direct it to a high-speed photodiode. The average photodiode signal was monitored along with the photodiode signal power spectrum using an RF/microwave spectrum analyzer. The alignment through the monochrometer was not optimized so that the spectra generated did not display the resolution of the instrument. However, they were sufficient for the purpose of checking the characteristics of the amplifiers and fiber gratings. The distributed feedback laser diode and the fiber Bragg grating both had operating points at approximately 1557 nm, well shifted from the peak of the amplified spontaneous emission of the Er-doped fiber gain medium.

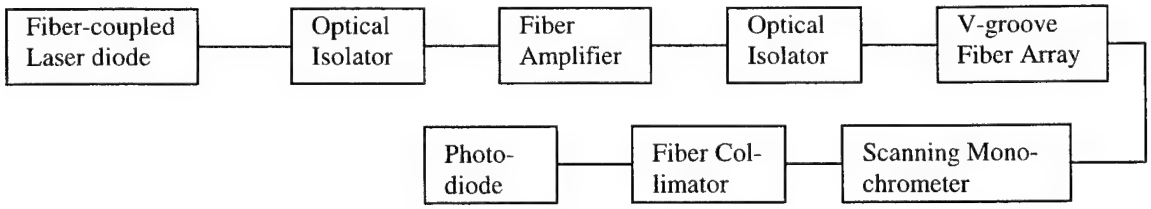

Figure 8(a) – Single-Pass Amplifier Configuration

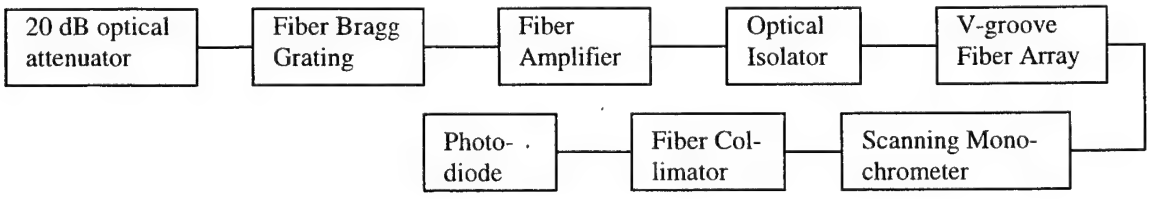

Figure 8(b) – Double-Pass Configuration

Figure 8. Schematic of the initial test apparatus used to investigate a single-pass (a) and double-pass (b) configuration using the fiber amplifiers.

Figure 9 shows how the spectra of the emission from the fiber amplifier changed with varying input signals from the laser diode while Figure 10 gives the spectra under feedback from the grating at two different pump levels. The pump level for the spectra in Figure 10 is approximately 1.5x laser oscillation threshold. In both cases the spectra was shifted from the amplified spontaneous emission spectrum of the free-running amplifier. Figure 9 shows how the amplified spontaneous emission is suppressed as the injected optical power is increased. The strongest optical signal is in the saturation regime as is shown by the relatively small increase in power of the output signal when the input is increased by a factor of five. In saturation, however, the amplified spontaneous continues to be further suppressed. Clearly, the two-pass configuration also produced sufficient feedback to overwhelm the spontaneous emission. There was even evidence of weak cavity effects in the form of small peaks in the photodiode output spectrum measured with the spectrum analyzer. This was due to the very weak feedback from the fiber couplers and optical isolator. Changing fiber amplifier elements, optical isolators, or V-groove fiber array elements produced changes in the detected optical output by up to approximately ±50%. Because the pump power to each amplifier element is under independent control, this level of variation can be readily compensated.

A full laser cavity was formed with two Bragg Gratings, as shown in Figure 11. A 10/90 optical coupler was inserted into the cavity to provide a control of the feedback from one grating and provide a means of coupling light out of the cavity. Additional attenuation within the cavity could be introduced by inserting either a 5, 10 or 20 dB fixed optical attenuator. Without the fixed attenuator there was a maximum roundtrip loss of 99% that was introduced by the fiber coupler in the configuration shown. A variable attenuator controlled the output level to a fast photodiode. This attenuator had one FC/PC fiber connector and so could not be inserted into the laser cavity where all other connectors were FC/APC. External optical injection could be provided by a laser diode signal injected into the fourth port of the fiber coupler. The signal from the fast photodiode was amplified and sent to a microwave spectrum analyzer. This allowed

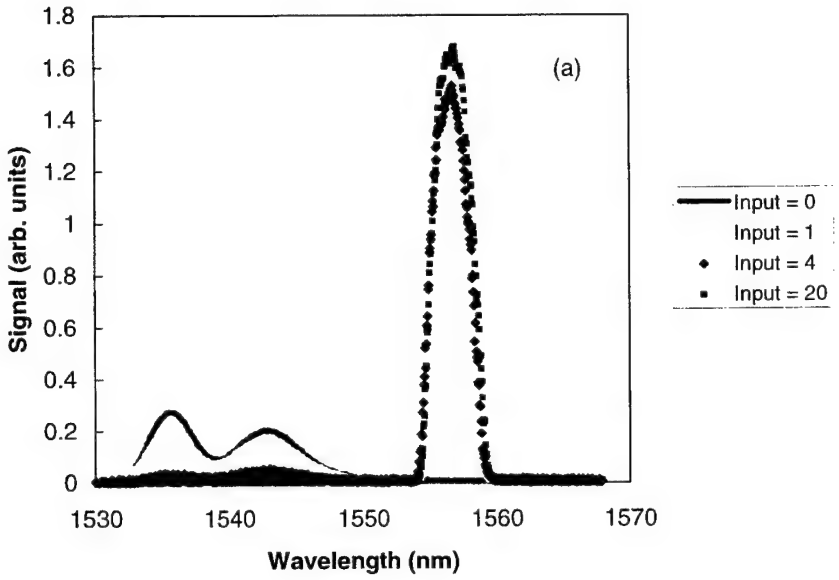

Figure 9(a) – Single Pass Amplifier Spectra.

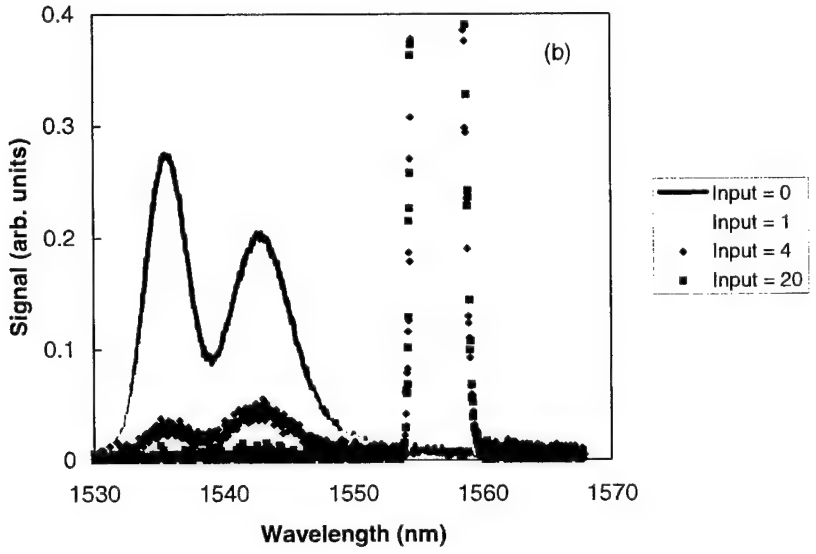

Figure 9(b) – Expanded scale spectra.

Figure 9. Spectra of the output of the fiber amplifier when subject to injection from a laser diode at 1557 nm. The laser input eventually saturates the output at an injection level near 1 mW and quenches the amplified spontaneous emission of the free-running amplifier. In (b) an expanded version of (a) is plotted to show the continued decrease in the amplified spontaneous emission signal in the saturation regime of the input signal.

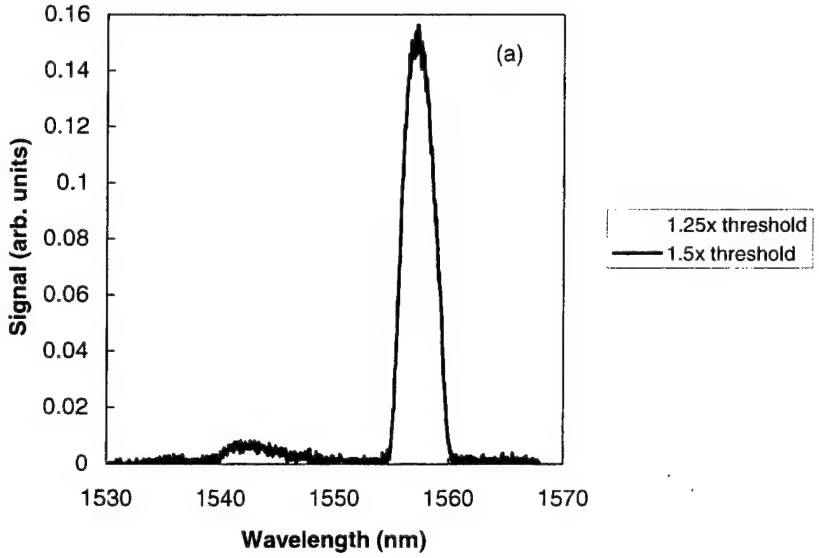

Figure 10(a) – Feedback Spectra.

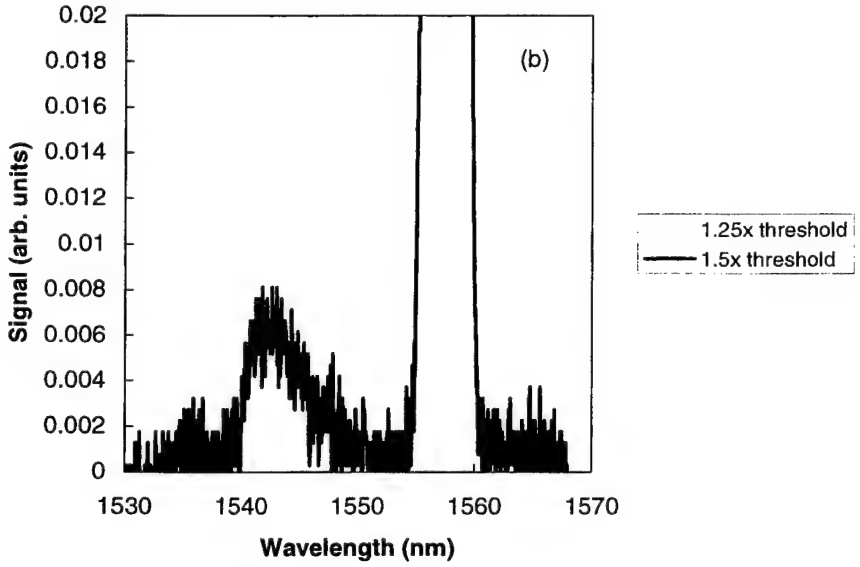

Figure 10(b) – Expanded Scale.

Figure 10. Spectra of the output of the fiber amplifier when subject to feedback from a fiber Bragg grating at 1557 nm. Two different pump levels are shown. The feedback peak grows relatively stronger than the amplified spontaneous emission peaks as the pump level is increased. In (b) an expanded version of (a) is plotted.

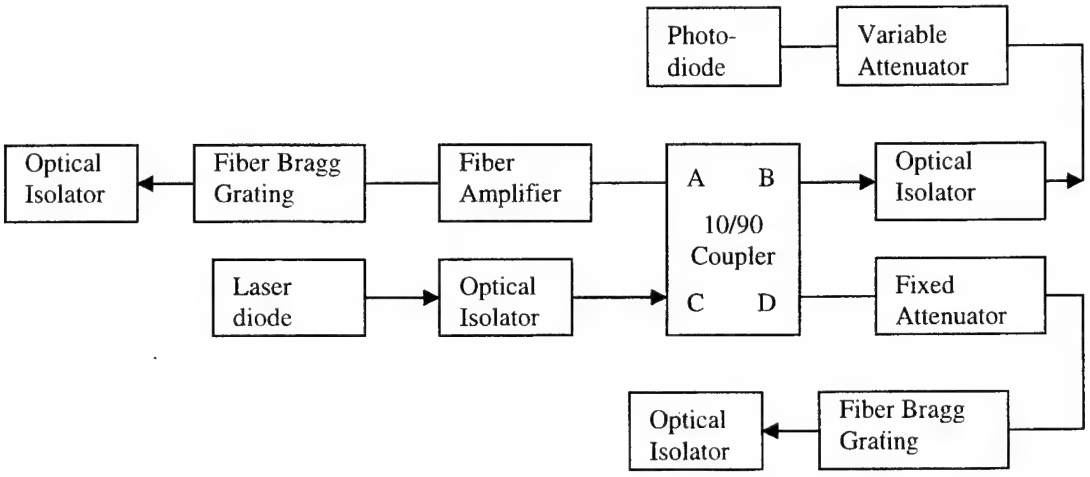

Figure 11. Schematic of a fiber laser formed with a fiber amplifier between two fiber Bragg gratings. The optical isolators prevent unwanted feedback into the cavity, The optical coupler provided a nominal 90% coupling between A(C) and B(D) and 10% coupling between A(C) and D(B).

investigation of the formation of a cavity between the two fiber Bragg gratings. We observed no evidence of the formation of a cavity, in the form of signal peaks at multiples of the inverse cavity round-trip time, with the 20 dB attenuator inserted into the cavity. Other spurious reflections were at least as strong as the –60 dB reflection from the 2nd Bragg grating/attenuator combination. With the 10 dB attenuator there were clear, but weak, peaks in the spectrum of the signal from the photodiode, at a spacing of approximately 8 MHz. The peaks had a linewidth on the order of a MHz. This indicated that a –40 dB reflection from the Bragg grating/attenuator was sufficient to be stronger than the spurious reflections. With the –5 dB attenuator, the peaks became relatively stronger and with no attenuator, the background signal from the amplified spontaneous emission was suppressed below the background noise level. This indicated that a reflected signal power of greater than –30 dB, probably on the order of –20 dB, was necessary to establish a dominant cavity for the fiber amplifier.

This is important for the intracavity coupling configuration, and particularly Talbot-type configurations. We have used a design criterion of a 250-μm spacing between fibers, dictated by what was readily available commercially. The mode diameter of the field launched from the fiber

is approximately 5% of this value. Because we have only four elements in the array and the fibers have a numerical aperture that spreads the power over significantly more than 1 mm in a Talbot distance, the fiber array may not launch sufficient power back into the respective laser cavities based on the observations above. However, the fiber collimator array significantly increased the launch diameter of the beam and reduced the numerical aperture.

We investigated the ability to generate a single-frequency output by injecting light from a single-mode DFB laser diode. Without optical injection, the fiber laser oscillated on many longitudinal cavity modes simultaneously. The fast photodiode that monitored the optical output through Port B of the 50/50 fiber coupler was connected to a spectrum analyzer. Figure 12 shows the beat signal between cavity modes. The mode spacing is approximately 6 MHz and there are strong signals beyond the 100^{th} harmonic. Note that some of the mode peaks appear to be doublets. This might arise from oscillating modes of orthogonal polarization.

When the laser diode was turned on, the multimode structure of Figure 12 vanished below the noise limit and the laser oscillated on a single mode at the injection frequency. However, the output was not steady in time. Figure 13 shows the temporal characteristics of the system under optical injection. Three output signals from Port B of the 50/50 beamsplitter are compared. The lower trace shows the output when the fiber laser is operated without optical injection. The upper trace shows the output when there is optical injection and the laser cavity is spoiled by disconnecting the FBG following port D of the 50/50 beamsplitter. At intermediate powers between these two traces is the trace of the optical output when the laser cavity is intact and an optical signal is injected. The signals are synchronized to the 60 Hz line current. Note that while the upper and lower curves are relatively steady, the middle curve fluctuates with a pattern that repeats itself in synchronism with the period of the line current oscillation. We verified that this fluctuation originated in the laser diode and not in the fiber amplifier. The observed output is consistent with the external injection frequency moving across cavity resonances. When the

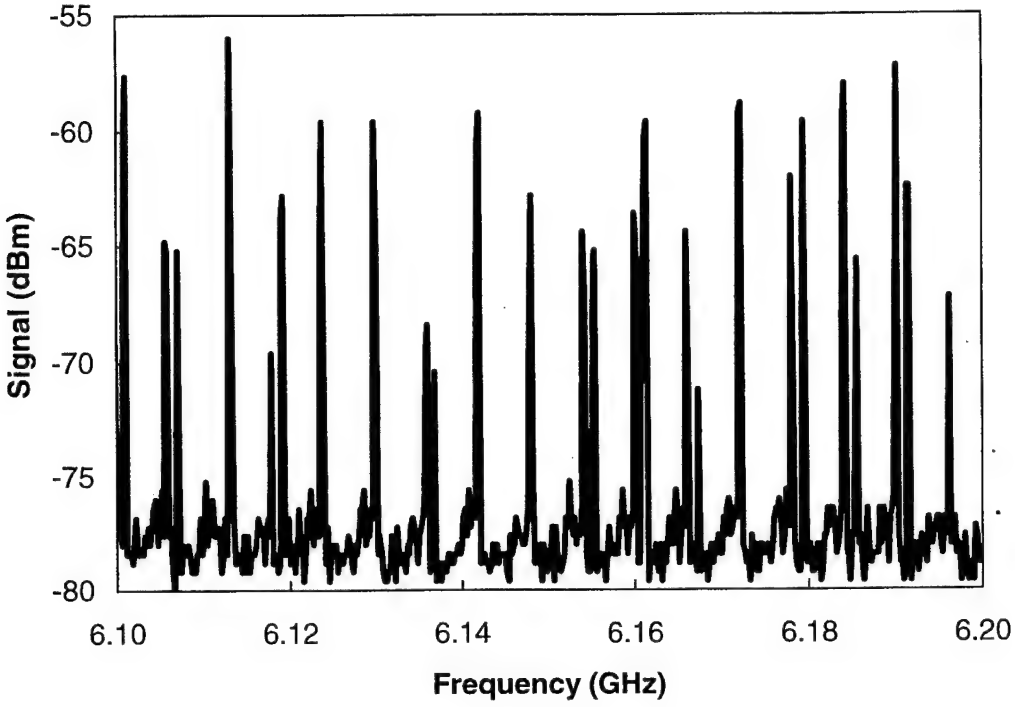

Figure 12. Cavity modes of the fiber laser. The mode spacing is approximately 6 MHz. Some of the modes show a double peak, indicating that possibly two orthogonal polarizations are oscillating simultaneously.

injected field and circulating field are in phase, the output power is highest because the circulating field in the cavity is highest. In previous measurements, we observed that the laser diode frequency shifted by approximately 350 MHz/mA so that a 6 MHz fluctuation corresponds to a current oscillation of less than 20 microamps. The optical signal is highest when there is no feedback because the presence of feedback clamps the gain at the threshold value so that the saturated output of a strong injection signal can be higher.

We found that we could insert an optical phase-locked loop that could compensate for the fluctuations of the laser diode using the output power of the fiber amplifier as the signal for the feedback loop. However, as thermal fluctuations slowly changed the cavity length points of negative feedback were transformed to points of positive feedback and locking was lost. Therefore, external injection locking will require more sophisticated control techniques.

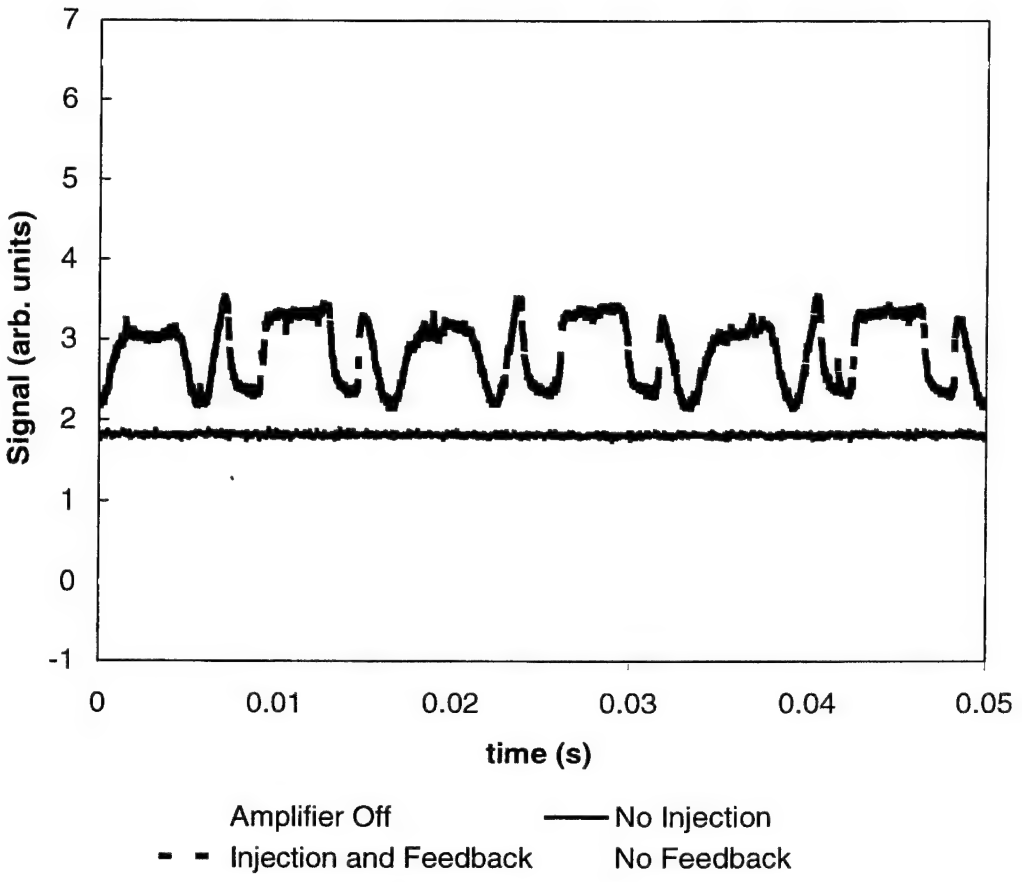

Figure 13. Output characteristics of the fiber laser under external optical injection. The Amplifier Off curve gives the signal level without optical output. With no optical injection the output signal level is given by the No Injection curve. With optical injection, the fiber laser output is given by the Injection and Feedback curve that fluctuates in synchronism with the 60 Hz line voltage. When the laser cavity is spoiled so that the externally injected optical signal undergoes single pass amplification, the output is given by the No Feedback curve.

The output characteristics shown in Figure 13 indicate that the optical injection must be phase matched to the cavity for optimal output. This is problematic in a fiber array because the individual cavity lengths cannot be matched with anything close to wavelength precision. We operated the fiber laser at approximately 1.6X threshold to obtain the data in Figure 13. The laser remained locked to the injected DFB signal even under out of phase conditions. However, at higher pumping levels, locking was not maintained.

We also investigated the characteristics of the eight-element fiber collimator array. We used the experimental configuration shown in Figure 14. The laser diode provided a monochromatic source for the experiments. Coupling up to the collimator array was done via optical fiber. The array launched the light into free space with the beam diameter approximately an order of magnitude larger than a bare fiber. The cylindrical lens collimated the light in the plane perpendicular to the one-dimensional collimator array and the 95% reflecting dielectric mirror provided feedback. A multimode fiber collimator collected light transmitted through the mirror. Several key results emerged from tests with this set-up. Two separate detectors are shown above the collimator array. Actually, there was only one detector that was connected to the appropriate point for measurements. From measurements with this set-up, we could conclude that on the order of 1% of the light was launched back into the collimator element from which it was emitted. The coupling fraction dropped off slowly for adjacent detectors so that more than 50% was coupled into elements offset by up to three. This should be sufficient coupling with sufficient cross coupling for the establishment of coherent emission. Complicating the situation, however, was the fact that the collimator array acted as a good reflector for light that was reflected off the output-coupling mirror but not launched back into the fiber. An optical cavity was created between the fiber collimator array and the 95% reflector. Such a cavity has been found to enhance the coherent coupling in a Talbot configuration [3]. However, it adds the requirement for wavelength-scale stability of the free-space part of the Talbot cavity.

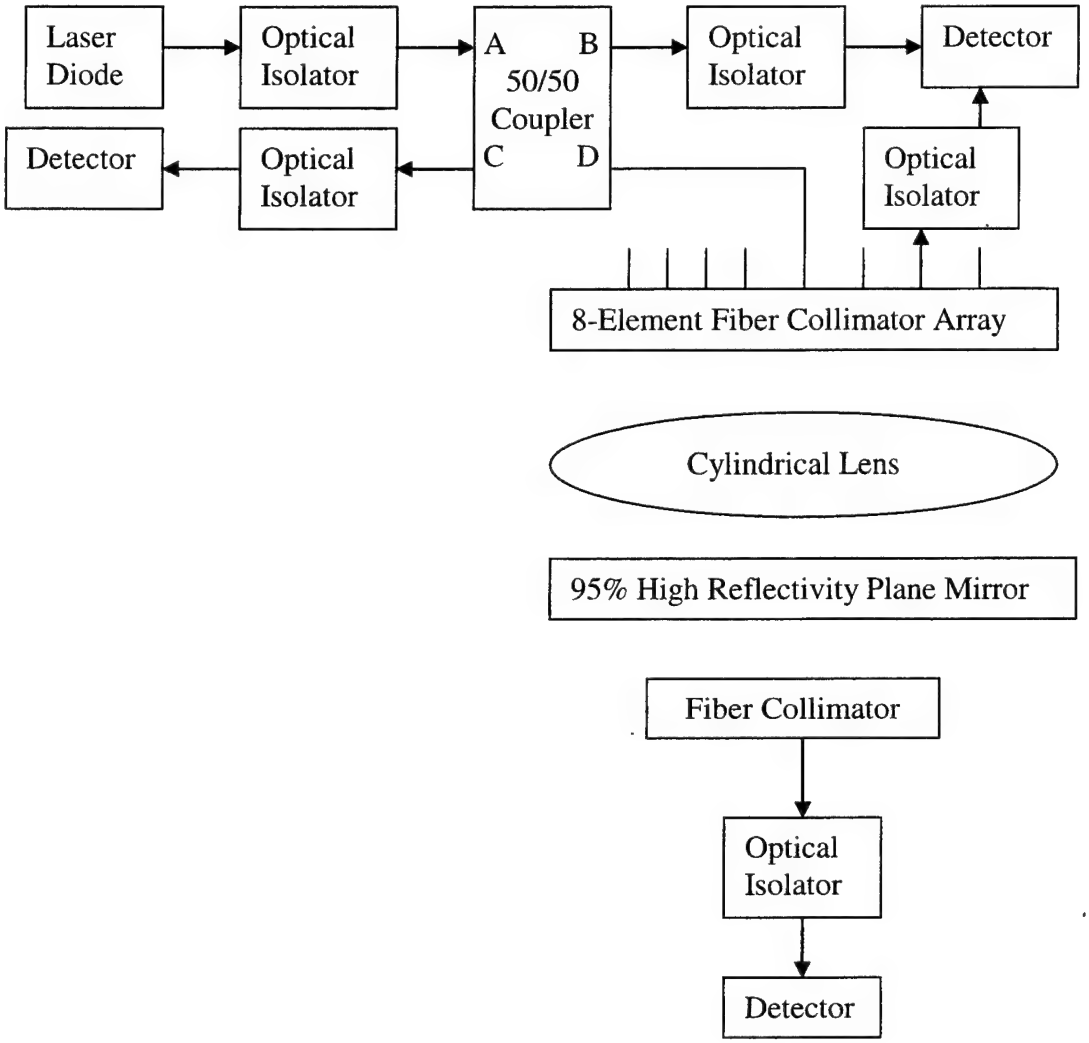

Figure 14. Schematic of experimental configuration to measure coupling into the free-space Talbot Effect region using a fiber collimator array.

COUPLED CAVITY CONFIGURATIONS

To understand some of the basic features of the coupling, the fiber laser cavity was initially defined by high-reflection fiber Bragg Gratings and output coupling was achieved with the use of fiber couplers. Previous work had shown that coherent coupling was possible using a cleaved, 2x2 fiber coupler, where the cleaved facet in the coupler interaction region was used as the common output coupler [3]. Because the small-signal gain of the amplifier is so high, up to 40 dB, we can be quite flexible in the insertion of intracavity elements. Figure 15 displays a two-element fiber laser that formed the basic apparatus of the tests performed this period. In this configuration, two fiber lasers are mutually coupled through the FBG after Port D of the 50/50 fiber coupler. In addition, an external optical signal can be injected into one of the two laser cavities through Port C of the 10/90 fiber coupler. In the 10/90 coupler, 90% of the power is passed from Port A to Port B and from Port C to Port D, and 10% of the power is passed from Port A to Port D and from Port C to Port B. The coupled cavity output is observed through Port B of the 50/50 coupler. We used a photodiode with a bandwidth of greater than 10 GHz. This detector also provided a signal proportional to the average output power that had a bandwidth of a few kHz. The external optical signal was either derived directly from a DFB laser diode or was amplified with a fiber amplifier. While the laser diode was current stabilized, there was some current or temperature jitter that caused small frequency fluctuations of the output. These fluctuations were synchronized with the line current that powered the laboratory electronics.

Using the commercially available components to create the configuration shown in Figure 15, the two laser cavities in the configuration had an optical path length difference of approximately 2.5%. The cavity mode spacing was approximately 6 MHz, or about 25 meters (physical path length times refractive index). If the 10/90 coupler is removed from the one cavity so that no optical injection is possible but the two cavities have the same high-reflector configuration, then the cavity lengths are matched to within 1 centimeter. A variation of on the order of 1 cm is the best possible using commercially available components.

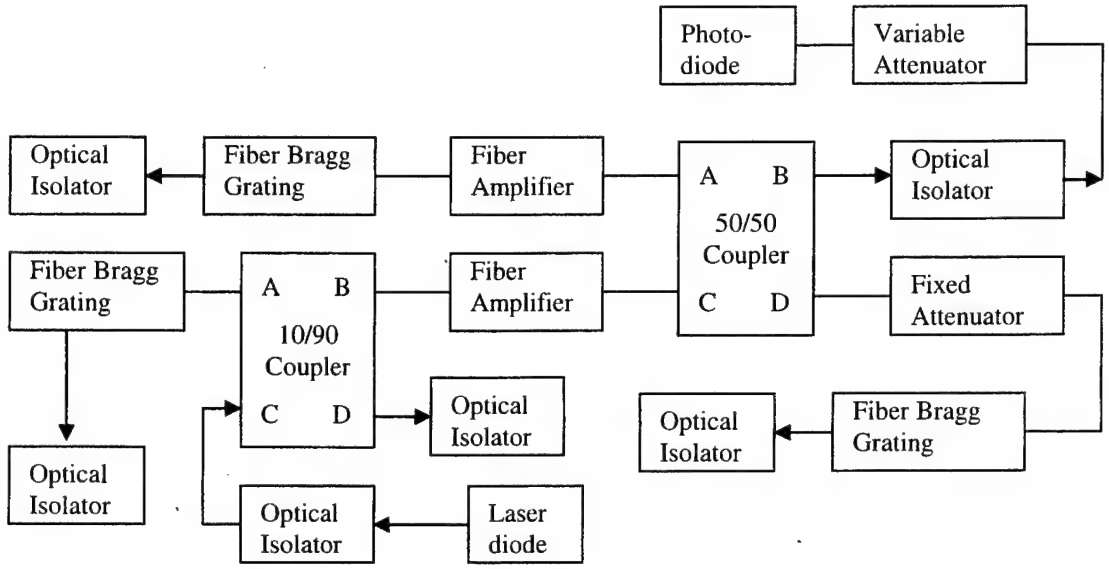

Figure 15. All fiber implementation of a coupled cavity built around two fiber amplifiers. Port B of the 50/50 coupler is the output while Port D leads to the fiber Bragg grating that provides mutual feedback. External optical injection can be provided at Port C of the 10/90 coupler.

Initially, the two fiber lasers were run in a mutually coupled configuration without external optical injection. Typical output characteristics are shown in Figure 16. When only one amplifier is turned on, there is a steady output at port B of the 50/50 coupler due to the above threshold operation of the solitary laser. When this laser is left operating and pump power is increased to the second amplifier, the following sequence of events is observed. The output power begins to drop and small fluctuations in the output power on the one to several second time scale are observed when the pump power is increased above the oscillation threshold for the second laser cavity. The power continues to drop as the pump power increases until a minimum is reached when the two cavities are pumped at approximately the same level. This is shown in Figure 16. Note that the fluctuations are now much longer than the period of the 60 cycle line oscillations. After the minimum is reached, increasing the pump to either amplifier increases the output power level.

When the output of Port D of the 10/90 output coupler is monitored, the output power monotonically increases as the power of the second amplifier is raised above threshold. When the pumping of the two amplifiers is similar, the power at Port D is nearly twice the power under single amplifier operation. This indicates that the mutually coupled lasers are configuring themselves so that the interference of fields at the 50/50 fiber coupler leads to minimizing the output and maximizing the intracavity circulating optical power. This was true both for the configuration shown in Figure 15 where the two laser cavities differed in optical path length by about 2.5% and when the cavity lengths were made as similar as possible, within 0.02%.

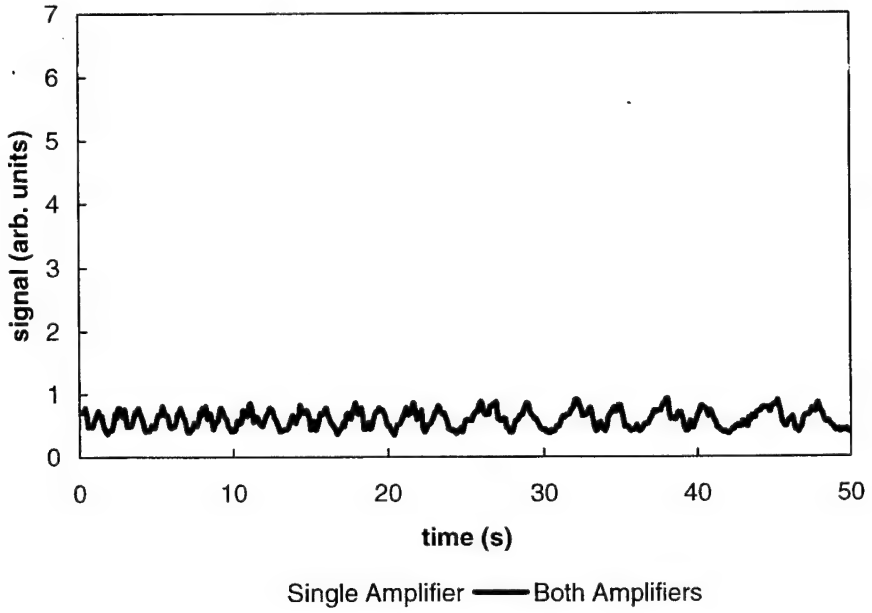

Figure 16. Output characteristics of the two-laser array. The upper curve shows the output from Port B of the 50/50 coupler when only one amplifier is powered. When the second amplifier is turned on, the detected power begins to drop when this amplifier pumping reaches the threshold for oscillation. The power drops steadily as the pumping of the second amplifier is increased until it reaches a minimum, shown by the curve labeled Both Amplifiers, when the pump level for the two amplifiers is approximately equal. The output power increases if either amplifier power is then increased further.

The propensity to coherently couple the two lasers is quite robust. The configuration was modified as shown in Figure 17. Now one laser cavity is strongly coupled to the FBG with the 90% ports of a 10/90 fiber coupler. The other laser is very weakly coupled, passing through 10% ports of two 10/90 couplers. This cavity is only marginally above the cavities formed by spurious reflections due to the intracavity FC/APC fiber connectors. However, the output signal at Port D clearly showed the coupling of the two laser cavities. The results are summarized in Table 1.

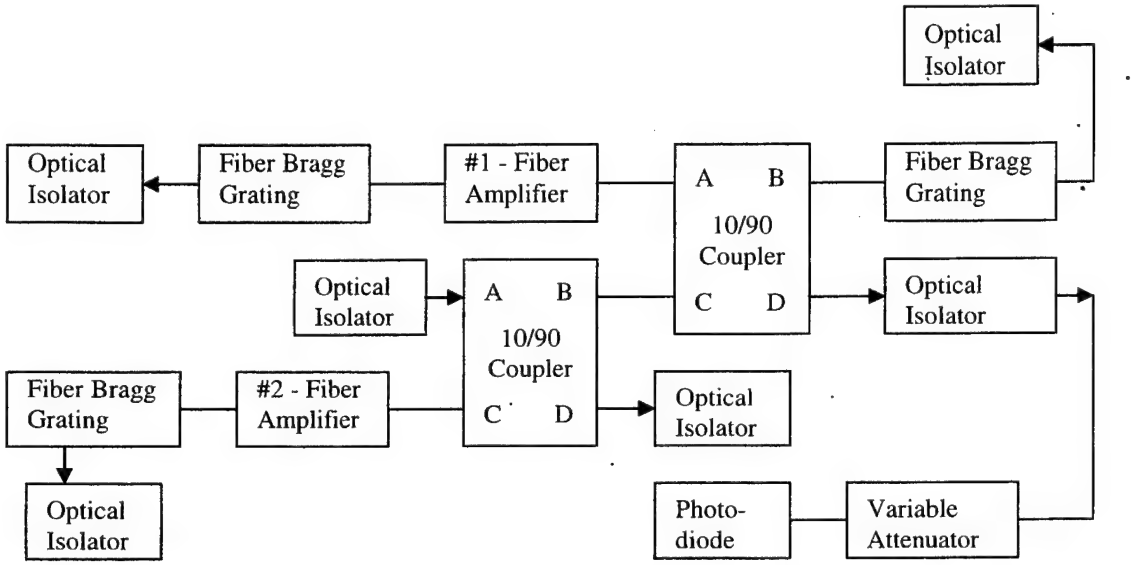

Figure 17. All fiber implementation of a coupled cavity built around two fiber amplifiers with asymmetric coupling to the fiber Bragg grating.

Table 1. Output power for the configuration in Figure 17.

Configuration	**Relative output power**
Laser with #1 amplifier alone	1
Laser with #2 amplifier alone	0.7
Simultaneous operation with equal pumping	Variable (0.53 – 1.48)

Under simultaneous operation the lasers never delivered an output power that would be consistent with incoherent summation. The power was always less. The variations in output

power occurred slowly, over a period of several minutes. They continued for the full duration of operation of the laser in this configuration, a period of over three hours. The weak feedback does not permit the cavity that uses amplifier #2 to strongly lock to the feedback signals at so its output phase fluctuates in response to environmental or operational changes. The feedback signal is dominated by the other laser cavity so that the phase relation between the two tends to drift over time. Nonetheless, even in this extreme case, there is still strong coherence between the two optical fields. The drift of the phase in this configuration may be relevant for the case of a large laser array. Similar to the case here for amplifier #2, only a small amount of the signal from an individual laser is fed back upon itself, while the summed injection signal from the other lasers in the array is much stronger. However, in the array case, the total feedback signal will be strong.

An additional modification of the apparatus was made to allow direct monitoring of the coherently combined output. Figure 18 is a schematic of the reconfigured apparatus. Now an uncoated fiber collimator replaces the FBG at the output end. The collimator was a commercially packaged unit consisting of a single-mode fiber and a GRIN (gradient index) lens. The uncoated face of the lens reflected about 4% of the light back into the fiber, forming an output coupling mirror. After a few centimeters of free-space propagation, the output from the collimator was launched into a second fiber through another collimator and then passed to a photodetector. As before, the output from the 50/50 coupler displayed the characteristics summarized in Figure 16. In contrast, the photodetector monitoring the collimator output displayed the characteristics shown in Figure 19. When both amplifiers are operating with similar output power, the coherently combined signal is detected through the collimator. The output power is approximately four times the power when either amplifier is operating individually. Almost all of the optical power in the cavity is passed to the feedback surface and little is directly coupled out of the 50/50 coupler.

A further example of the coherent coupling is shown in Figure 20 for this two-laser configuration. The photodiode voltage for the two monitoring photodiodes shown in Figure 18 is plotted as a function of the bias current to the pump laser diodes used to one fiber amplifier. In

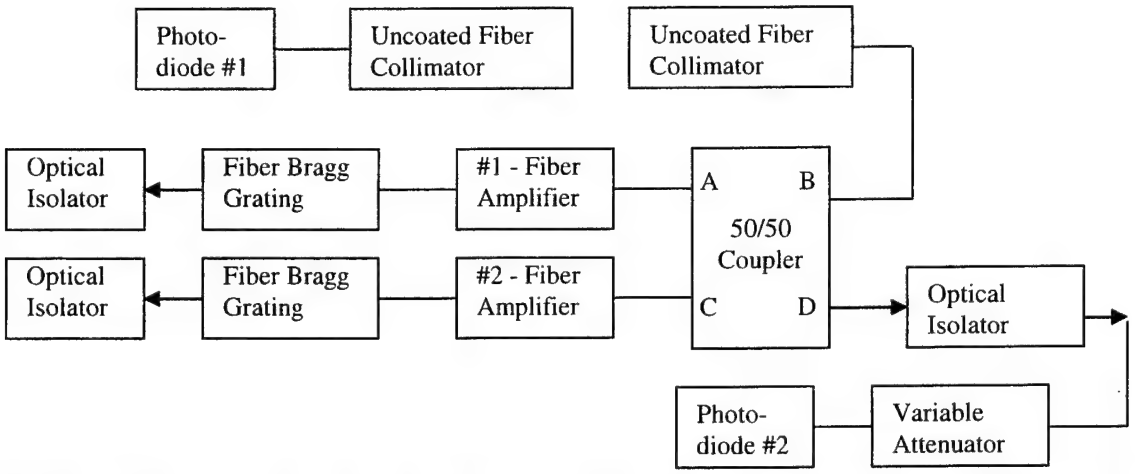

Figure 18. Modification of the coupled fiber laser to allow the monitoring of the output of the mutual-coupling reflector (output coupler).

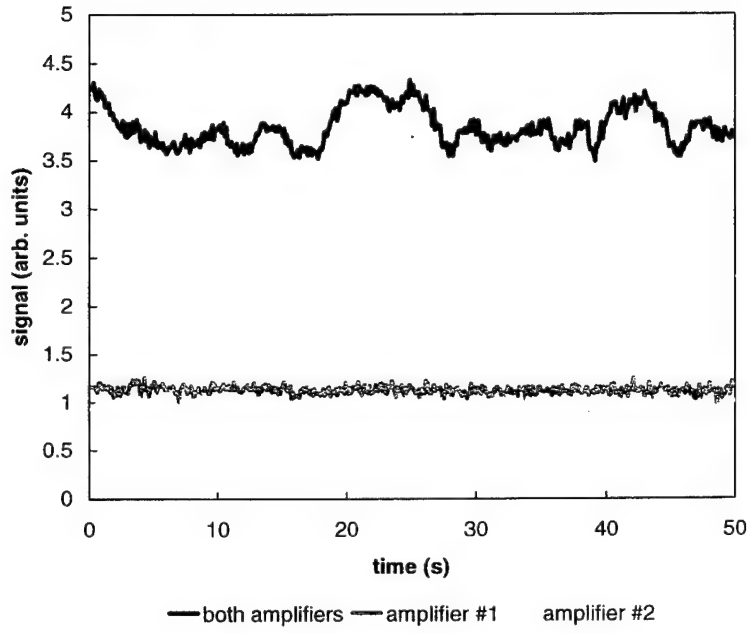

Figure 19. Output characteristics of the two-laser array shown in Figure 18. Power is monitored by the photodiode following the fiber collimators. The collimator after the amplifiers acts as a common output coupler for the two laser cavities. The second collimator simply recollects the light into a fiber for transmission to the detector. When both amplifiers are operated under similar pumping the light is preferentially coupled into the collimator arm of the 50/50 coupler.

Figure 20(a), the amplifier is run in isolation and the photodiode signals grow proportionately, showing nearly equal splitting of the output at the fiber coupler. In Figure 20(b) the other amplifier is pumped above threshold so that it causes photodiode signals corresponding to nearly equal outputs without pumping of the original amplifier. Then, as the pumping to this amplifier is increased, the signal to the photodiode monitoring the output at the collimator grows much more rapidly and the other photodiode signal goes through a minimum. The minimum occurs when the two amplifiers are pumped to a similar output level. Note that the signal measure by photodiode #1 is now approximately four times, not two times, the single laser signal. In this case almost all of the power is coupled to the output port for the fiber collimator. This maximizes the feedback signal into the cavity, maximizes the circulating power level, and minimizes the inversion density.

Figure 21 shows typical optical spectra for two of the laser elements operating independently and when operated in the mutually coupled configuration. The other two amplifiers were turned off for this test. Because the high reflection bandwidth of the FBGs is approximately 100 GHz, only part of the optical spectrum is shown. The laser oscillates on several modes simultaneously but these modes are coming and going continuously on a time scale on the order of one second. Again, this time scale is consistent with small environmental, i.e. temperature, changes in the laboratory. The random switching of power between modes appeared to be somewhat faster in situations where two or four elements are coupled together, but still consistent with environmental fluctuations.

Because each laser in the array has a slightly different cavity length, the mode spacing changes when the lasers are operated in a coupled configuration. Figure 22 shows a detail of the power spectrum of the photodiode signal showing an individual mode beating frequency. Note that the frequency of the peak for the two individual lasers is offset and that the peak of the locked two-laser system lies in between. The mutual locking causes the oscillation frequency to be pulled away from the natural oscillation frequency of the solitary cavities. This mode beating frequency corresponds to the 79^{th} harmonic of the fundamental mode frequency and the offset between the two frequencies of the isolated lasers corresponds to a fractional cavity-length mismatch of approximately 0.0008.

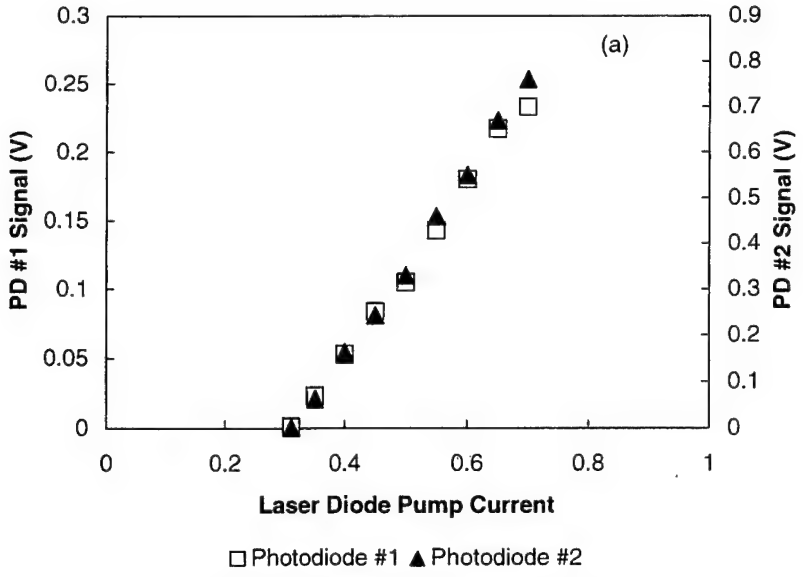

Figure 20(a) – Single Amplifier output.

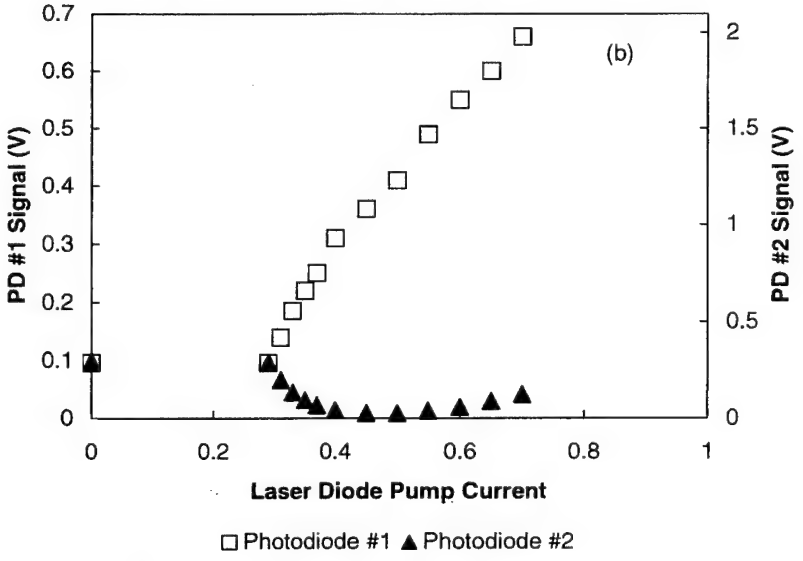

Figure 20(b) – Dual Amplifier output.

Figure 20. Output characteristics of a two-amplifier configuration. Figure 20(a) shows the output measured by photodiodes #1 and #2 when one amplifier is operated by itself. Figure 20(b) shows the signals when amplifier the second amplifier is first pumped above threshold to the output level shown at the zero current condition. Note the difference in scales between (a) and (b).

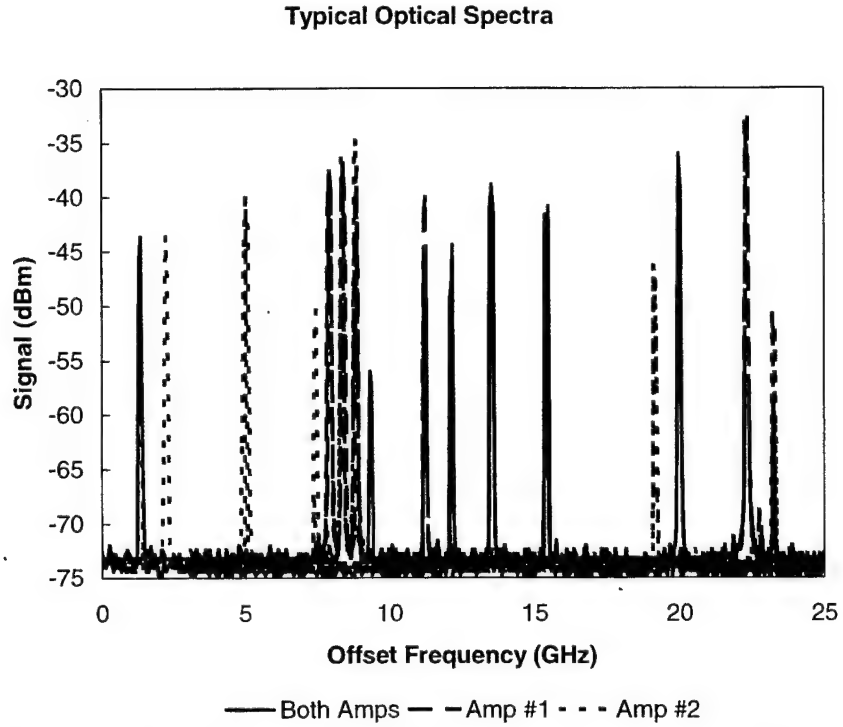

Figure 21. Partial optical spectrum of two of the fiber laser elements of the array operating independently and operating in a mutually coupled configuration. Each peak may correspond to several optical modes due to the measurement resolution of approximately 100 MHz and the mode spacing of approximately 6 MHz.

We also investigated the mutual coupling characteristics of a two-laser system when one of the two lasers was injection locked to an external optical signal. An optically isolated DFB laser generated the external optical signal. While the laser diode was current stabilized, there was some current or temperature jitter that caused small frequency fluctuations of the output. These fluctuations were synchronized with the line current that powered the laboratory electronics. As reported last quarter, the jitter caused the locking to produce a fluctuating output power from the locked fiber laser as one of its free-running mode frequencies came into and out of resonance with the master laser. The second laser did not, in general, coherently couple with the injection-locked laser but appeared to maintain its free-running laser characteristics. Tied with the other results, it appears that the explanation for the coherent coupling is that the array operates with the particular modes that can mutually lock together to produce the highest circulating optical

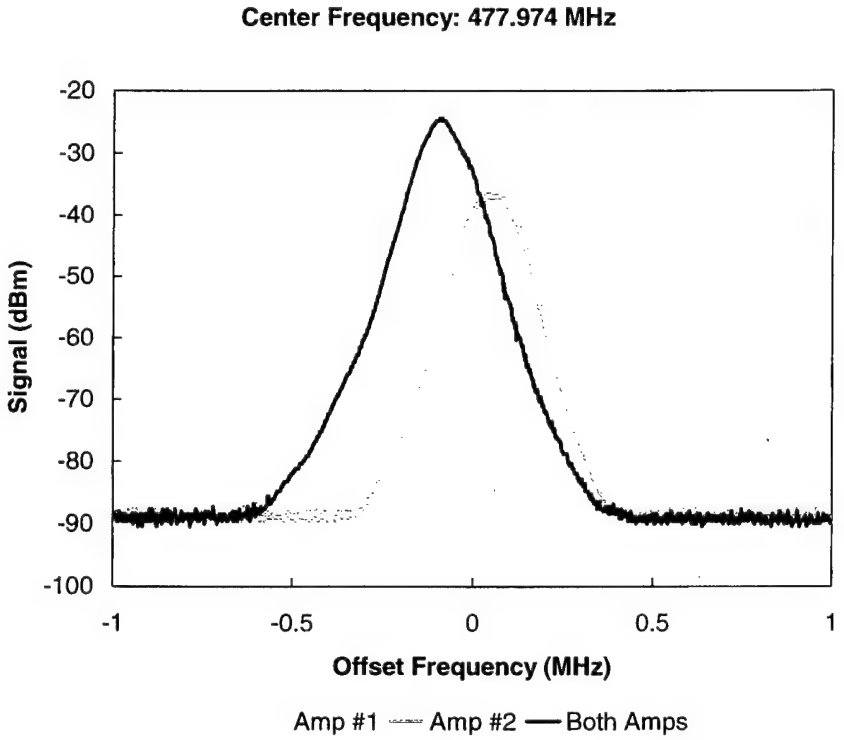

Figure 22. Mode beating spectrum of the 79th harmonic of the fundamental mode frequency. The frequencies of the two isolated lasers are offset and the coherently coupled laser frequency is between the two frequencies showing the frequency pulling of the mutually coupled interaction.

power, lowest inversion level. When there are only two lasers, this is relatively easy to accomplish, even with a cavity mismatch, due to the large number of modes within the high reflectance frequency range of the FBGs.

Figure 23 displays the full four-element fiber laser array that formed the basic apparatus of the tests performed this period. In this configuration, each fiber laser has an FBG as a high reflecting end mirror. These FBGs are commercially available products manufactured by Corning and specified to operate as a high reflector on one of the 100 GHz wide channels of the ITU grid. The gratings used in these experiments were fabricated for the grid channel at 1557 nm. A cladding-pumped, Er-doped fiber amplifier provides gain to each laser element. Separate pumping to each amplifier is provided by laser diodes under independent bias control. Each element has

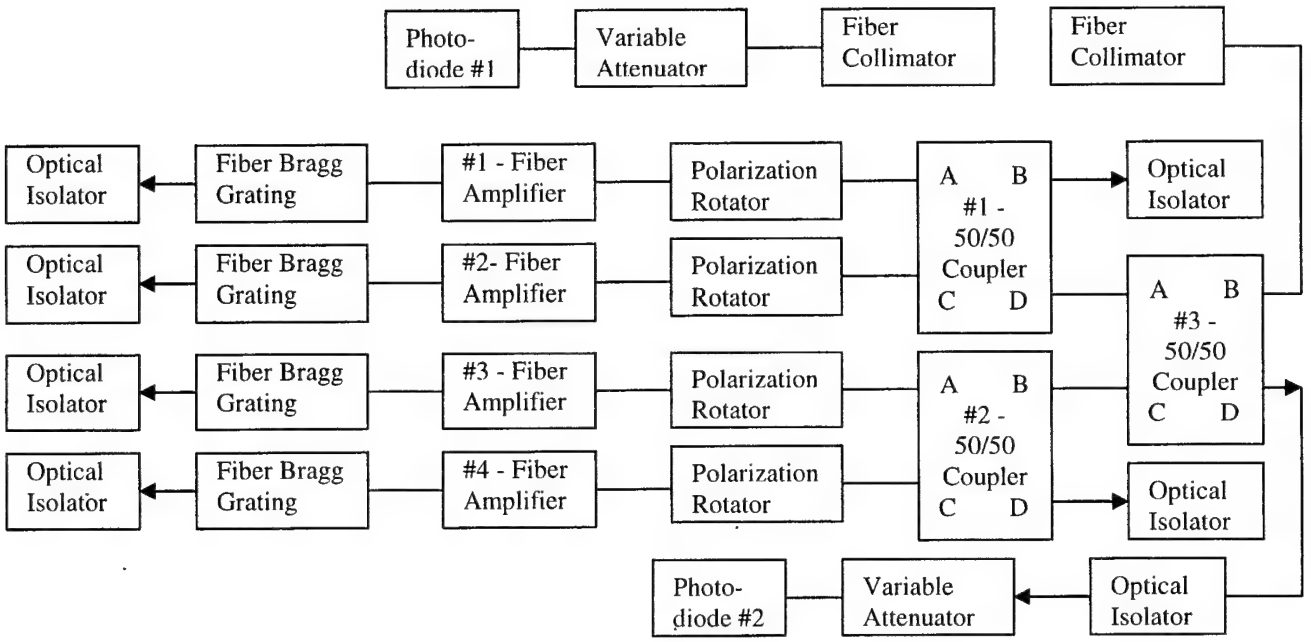

Figure 23. Schematic of the configuration of the fiber apparatus into a four-element mutually coupled array. Each element in the array has an independent fiber Bragg grating end reflector, Er-doped fiber amplifier, and polarization rotator. Mutual coupling is achieved through two layers of 50/50 fiber couplers. A flat, uncoated endface on a fiber collimator that is at one output port of the final 50/50 coupler, port B of coupler #3, acts as a common output coupler for the array. Output coupling is also possible through the other port, port D, of the same 50/50 coupler as well as port B of coupler #1 and port D of coupler #2. Optical isolators prevent stray back reflections into the cavity. One photodetector monitors the output through the fiber collimator. A second photodiode can be positioned at any of the other output ports. The photodiode signals are monitored with oscilloscopes and a microwave spectrum analyzer.

independent polarization control. During this period it was found that alignment of the polarization axes of each of the elements was critical for coherent coupling. With two lasers, the polarization alignment could be achieved by simply twisting a fiber and clamping it down. This imprecise control was not adequate when four lasers were used and polarization control elements were purchased from Newport Corp. These elements operate on essentially the same principal as the simple twisting technique but are manufactured to have much more precise control. Only three polarization controllers are required, but four can be used to more precisely match cavity length. A tree of 50/50 fiber couplers, also purchased from Newport Corp provides mutual coupling of the lasers. The feedback element/ output coupler for the cavity is provided by the end face of a fiber collimator that is connected to port B of coupler #3. This uncoated face provided about 4% back reflection into the cavity. Because the small signal gain in the cavity can be made to be greater than 40 dB, the output losses and parasitic losses can be easily overcome.

There are three other output ports for the array at the unused output ports of the 50/50 couplers. As previously reported, coupling here is minimized under coherent operation. Various photodiodes were used to monitor the output at both the output coupler and the excess coupling points of the three 50/50 couplers. One had a bandwidth of greater than 10 GHz allowing broadband spectra to be generated in combination with a microwave spectrum analyzer. This detector also provided a signal proportional to the average output power that had a bandwidth of a few kHz.

Figure 24 shows the temporal characteristics when four lasers are operating and compares the output through the fiber collimator that acts as the cavity output coupler when one laser is operating with the case when four lasers are operating, each at approximately the same input power level. When only one laser is operating the 50/50 couplers act as loss elements for the cavity. The output power through the fiber collimator is only approximately 25% of the power generated after the round trip pass through the amplifier. However, when all four lasers are operating, the lasers tend to operate so that their phases at the 50/50 couplers lead to destructive interference on the parasitic loss ports and most power is directed to the fiber collimator output coupler. If the four lasers are each pumped to the same level, then, in theory, these losses can be

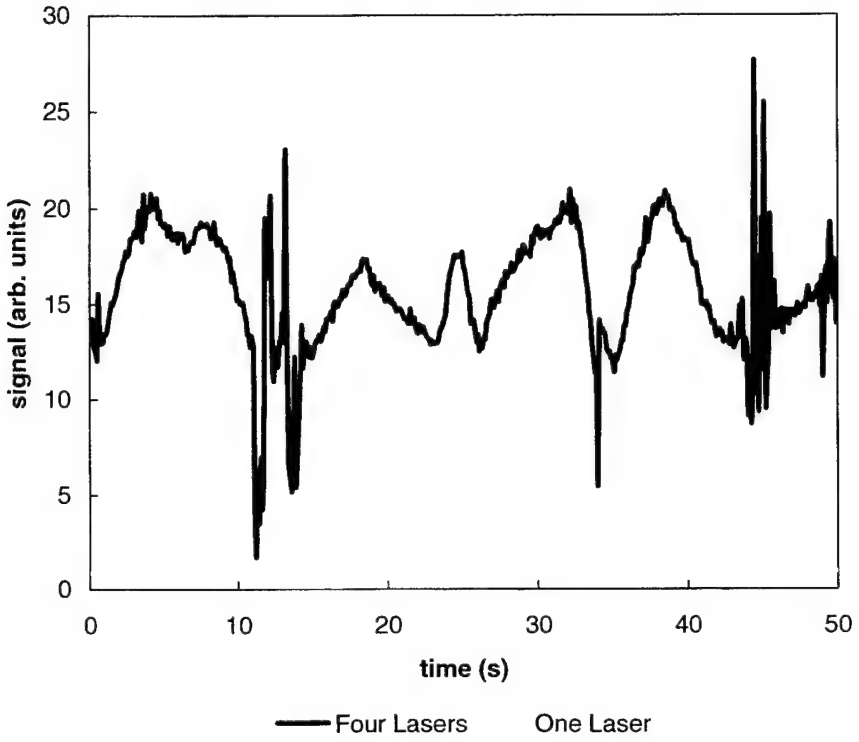

Figure 24. Average output power from one laser in the array when operated with the other amplifiers unpumped, and with all lasers pumped to produce equal output powers when operated alone. If the lasers combined incoherently, the four-laser array should operate with four times the power of the single laser. Due to coherent coupling, however, the output power is considerably higher. Slow time variations, on the order of seconds occur due to environmental changes in the laboratory. More rapid fluctuations indicate that the array had switched to an unstable condition where the output power varied on a sub-microsecond time scale.

essentially eliminated. In Figure 24 we observe that the combined power from four lasers is much greater than a factor of four larger than the single laser output. It is close to the 16x larger that would be expected if there were no losses at the couplers.

The coupled-laser output in Figure 24 shows strong variations with time. These variations are much larger than the two-amplifier coupling case, as reported last quarter. The variation in the

output power of the coupled array typically occurred on a time scale on the order of seconds. Observations with higher temporal resolution showed that the average power was always fluctuating on a sub-microsecond time scale. Periodic fluctuations with frequency of the laser cavity mode spacing or one of its harmonics could often be identified. Also, for short time periods, the laser entered an operating condition where the output power showed a spiking output with a repetition frequency that varied in the range of 30-50 kHz. This frequency range corresponds to the relaxation resonance regime. Examples in Figure 24 are at approximately 12, 14 and 45 s..

The photodiode signal power spectra from the four-element array showed wide variations during the investigation. Initially, we observed spectra like that shown in Figure 25. A free-running single laser always had a sparse mode-beating spectrum where the individual peaks varied in a random fashion. In contrast, the coupled laser system showed a dense mode-beating spectrum that extended over hundreds of MHz. Later, however, the spectra changed to the characteristics shown in Figure 6. Now, the lasers all displayed a mode-beating pattern with peaks at approximate multiples of 500 MHz. Subsequently, the coupled laser system showed a much narrower band of mode beating frequencies than before, as shown in Figure 26, and details of its low-frequency components are shown in Figure 27. Nonetheless, there was always some broadening of the mode-beating spectrum of the coupled laser system relative to the single laser system. The appearance of the approximately 500 MHz frequency spacing possibly indicates that some intra-cavity reflection point has developed. However, we have not been able to isolate it. Based on the spectral characteristics of the coupled laser output, we concluded that the lasers operated on a relatively small number of optical modes or mode clusters, on the order of 10. The degree of coherent coupling depended on how well all four of the lasers could be induced to oscillate on frequency-pulled modes of the same frequency. Because the laser cavities differed in length by 1 cm or more, the frequency overlap of the different modes was random and the probability of overlap could be expected to become ever more difficult as the number of laser elements increased. This would explain our observations.

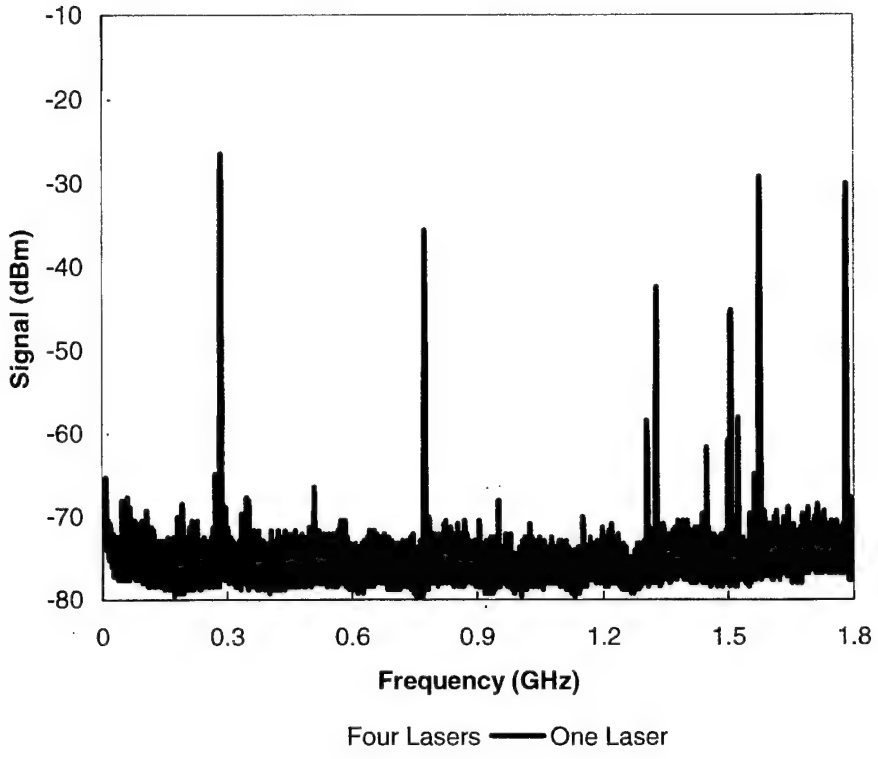

Figure 25. Mode beating spectrum of the fiber array when operated in the coherently coupled state and when one laser is operated in isolation. The single laser has a sparse mode-beating spectrum at low frequencies while the coupled system displays a dense mode-beating spectrum.

In an attempt to improve the coherent coupling performance, we tried some modifications to the basic laser array. We moved two of the four polarization control elements to the other side of the tree of fiber couplers. The rationale behind this was that the polarization controllers would slightly change the length and refractive index of the fibers, as well as the polarization, and that this characteristic might be useful at each stage of the fiber combination. However, this effect, if it existed at all, was too small to produce any measurable change on the output characteristics of the four-element array. The coherent coupling did not improve. Note that this configuration causes the lasers to have different cavity lengths by approximately 10 cm. This did not appear to have a significant effect on performance either.In a second experiment, we modified the pump current to the laser diodes that pumped the Er-doped fiber gain medium of one of the four lasers.

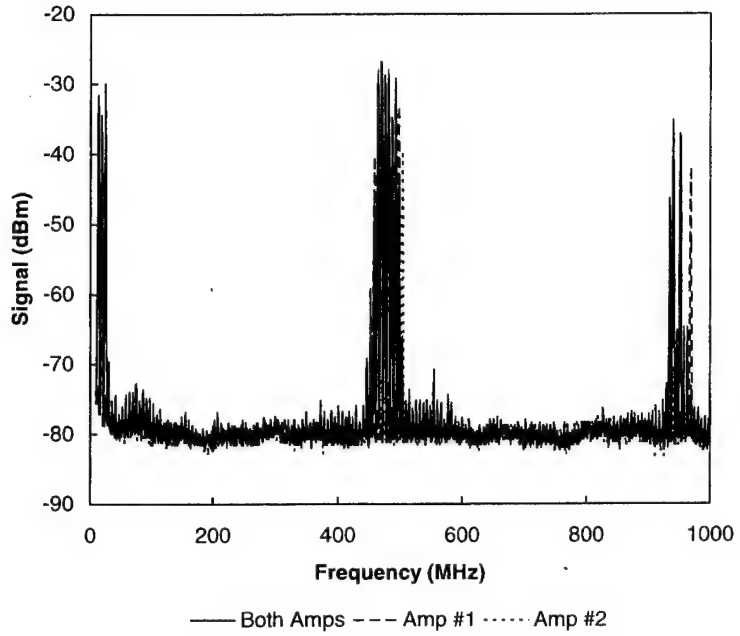

Figure 26. Mode beating spectrum of two isolated lasers and of the two laser when coupled together. The new frequency structure at multiples of approximately 500 MHz is possibly due to a parasitic reflection point within the laser cavity.

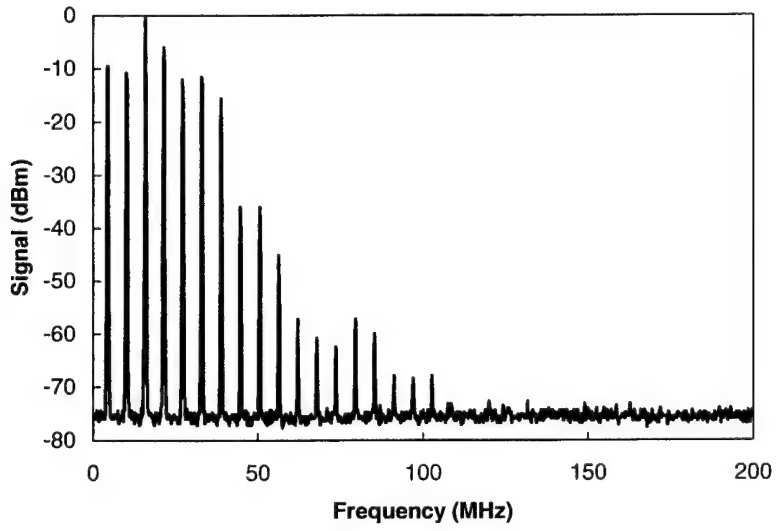

Figure 27. Low Frequency mode beating spectrum of the coherently coupled four-element array corresponding to Figure 26. Note that it is much narrower than the spectrum measured under nominally similar conditions in Figure 25.

Instead of dc pumping, we pumped the laser diodes at a frequency that matched the relaxation resonance frequency of the isolated fiber laser, between 30-50 kHz. We had the following rationale for this test. We had previously observed that the mode frequencies had a jitter of between 10-100 kHz under dc operation when we monitored the power spectrum with the microwave spectrum analyzer. Forcing the laser to oscillate at the relaxation resonance frequency would split the mode frequency into a comb of frequencies separated by the resonance frequency. It was hoped that the comb of frequencies might produce a better probability of locking by increasing the probability of spectral overlap between lasers. We did observe that the relaxation oscillations forced on one laser were propagated to all lasers in the array. However, the average coherent output from the array did not improve by this technique.

In a third experiment, we attempted to observe evidence of Stimulated Brillouin Scattering (SBS) within the array. We have postulated that the optical nonlinearities in a fiber might play a role in the spectral characteristics of the laser output. The SBS signal is the nonlinearity with the lowest threshold for a narrow frequency pump beam. At 1.55 micrometers wavelength, the SBS signal is expected to be approximately 10 GHz below the pump signal. To enforce narrow frequency oscillation, we injection locked a fiber laser to the output of a DFB laser diode. The locking was not complete, but the output at the injection frequency was the strongest spectral component. We observed no particular enhancement at offsets approximately 10 GHz lower frequency. Most likely, this was due to the relatively low power levels, < 100 mW, circulating within the laser cavity. Further investigations will require either more powerful amplifiers or significantly longer laser cavities.

CONCLUSIONS

Coherent coupling of fiber lasers has been proposed as a means to generate efficient, compact, high brightness, high power lasers. Previously, it was demonstrated that coherent coupling of two fiber lasers could be achieved when one half of a 2×2 fused taper single-mode fiber coupler was used as the beam combining and output coupling element by cleaving the center of the coupling area [1]. Here, we have demonstrated that cleaving of the 2×2 fiber coupler is not necessary. If cavity feedback is placed after one of the output ports of the coupler, the two fiber lasers will self-organize their optical output to minimize the power that is coupled to the other output port. By doing so, the fiber lasers maximize the circulating optical field within the laser cavity and minimize the inversion of the gain medium.

We have demonstrated this effect by constructing a flexible demonstration apparatus using commercially available components. Fiber lasers, each with an independently controlled Er-doped fiber amplifier and a fiber Bragg grating that is specified for the same 100 GHz element of the ITU grid, are intracavity coupled using a standard 2×2, 50/50 fiber couplers. One output port is coupled to an uncoated fiber collimator. The flat face of the collimator acts as a common output coupler for all the laser cavities in the array, providing feedback to the amplifiers. The other output port is a cavity loss that depends on the coherence of the circulating optical fields. The output from both the fiber collimator and the loss port are monitored. Care is taken to insure that external feedback into the cavity is insignificant. In the system constructed, the cavity mode spacing is approximately 6 MHz. For these measurements, the lasers were operated at low power levels so that nonlinear effects such as stimulated Brillouin scattering and self-phase modulation were unimportant. All fiber is of the single-mode, non-polarization preserving type.

The transmission characteristics of a 2×2 coupler depend on the characteristics of the incident light fields. When only one amplifier is operating, light is incident from only one port and is transmitted through both output ports. However, as the pump power to additional amplifiers is raised above threshold, the power can be asymmetrically coupled into the output port connected to the common output coupler. The output power through the loss port begins to decrease as the

pumping to a second amplifier nears threshold. In a two laser configuration, when the pumping of the two amplifiers is similar, almost all power is coupled through the port to the common output coupler and the detected output power is approximately four times the single laser result. Further increase in the pump current shows that some power is transmitted through the loss arm but that the coupling is strongly asymmetric. The mutual coupling of the two lasers did not induce polarization self-alignment. Typically, one of the two fibers would have to be stressed to rotate the polarization into alignment to achieve the greatest asymmetry of coupling.

A key factor is that the cavity lengths of the fiber lasers in the array cannot be matched under realistic conditions. Under coherent operation, there was frequency pulling of the cavity modes to generate mode by mode coherence. The cavity length of the lasers was varied and coherent coupling was observed for length mismatches as large as approximately 2.5%. Even with fairly large length mismatches, due to the large number of cavity modes there will still be several in the spectra of the free-running lasers with nearly overlapping optical frequencies. Optical spectra taken with a resolution of approximately 100 MHz showed that a sparse set of modes or mode clusters, on the order of 20, oscillated over the 100 GHz bandwidth of the fiber Bragg gratings.

In this configuration, coherent coupling of the two fiber lasers minimizes intracavity losses, and maximizes the power fed back into the cavity from the fiber collimator output coupler. This feature allows cascading of the coupling scheme to a large number of lasers to achieve high coherent output power. However, due to cavity length mismatches, scaling is complicated by the phase mismatch. It becomes more difficult to find common mode-frequency overlap among many cavities with different lengths. Experiments with a four-cavity array show less complete coherent coupling and greater sensitivity to fluctuations in laboratory conditions. Therefore, this system may not scale to high power levels without the addition of cavity length (phase) control of the individual laser cavities.

The Talbot cavity configuration would be subject to similar considerations. In the Talbot cavity the situation is further complicated by the fact that there are many combinations of the phase of the individual emitters that will give rise to coherent output. The relative difference in the

coupling between these different phase configurations is relatively small so that the desired in-phase mode of the Talbot cavity will be even harder to maintain than it is in the case of the all-fiber intracavity coupling.

RECOMMENDATIONS

Laser cavities have lowest losses at discrete frequencies that are defined by the optical path length of the cavity. These frequencies produce the in-phase condition for laser oscillation after one round trip in the laser cavity. Fiber lasers, with optical path length typically of 10 meters or more, can be matched in path length to ±1 cm. Such length mismatch will guarantee that the oscillation frequencies of different lasers do not match and that there must be frequency pulling, and phase mismatch, across an array for coherent coupling. Because of the relatively small frequency spacing of laser cavity modes, 16 MHz for a 10-m optical path length, there will typically be many modes within the useful bandwidth of the gain medium and/or reflectors. Therefore, random near-resonances will occur. With a small number of lasers, self-configuration into these near-resonant modes is possible. However, as the number of lasers increases, it becomes increasingly difficult to force all of the lasers to oscillate in near-resonant modes. We have observed that when four lasers are coupled that the coherence is lower and that the sensitivity to environmental fluctuations is stronger.

Therefore, a mechanism for length or phase compensation or control is required if this intra-cavity coherent coupling technique is to be successfully employed to coherently combine multiple fiber lasers. One could envision the insertion of individual electro-optic phase controllers in each laser cavity, with monitors at the loss ports of the 2×2 couplers, and actively controlling the phase of the laser output. Such techniques have been employed to coherently combine arrays of laser diodes [5]. However, this adds considerable complexity and cost to the laser circuit. Therefore, it would advantageous to implement self-organization of the optical phase to allow a better match of the different oscillation frequencies of the different lasers.

Fiber nonlinearities offer a potential mechanism for the self-organization of the cavity optical phases to maximize coherent coupling. Though relatively weak, the nonlinearities have been exploited to generate a variety of useful characteristics including optical pulse compression and stretching, soliton pulse formation, and wavelength shifting [6]. The long interaction lengths over which high-intensity optical fields can be maintained in optical fibers compensate for the small

nonlinear optical coefficient. Even with relatively low power levels, high intensities can be achieved when the beam is confined to single-mode propagation in a fiber. Single mode cross sections of 5×10^{-7} square centimeters (cm^2) are typical, yielding megawatt per square centimeter (cm) intensity levels for Watt (W) incident power levels. Interaction lengths of kilometers (km) are possible, particularly in the low-loss, 1.55-μm spectral region.

There are several nonlinear optical interactions that can play a role in modifying the index characteristics of the fiber medium. All optical fiber has a background nonlinear component to the refractive index. While weak, its effects on the refractive index can be sufficient to introduce significant phase changes over sufficiently long path lengths. This nonlinearity has an effectively instantaneous response time and yields an index change at a point in the fiber that is proportional to the instantaneous intensity of the circulating optical field. In a frequency-based (Fourier transform) description, this yields self- and cross-phase modulation of the different frequency components. Coefficients for this nonlinear process are typically on the order of 2 $W^{-1}km^{-1}$ in the 1.55-μm spectral region [7]. Typically, no energy is exchanged between the optical fields and the fiber in this interaction. However, impurity absorption is possible and saturation can be considered. In contrast, stimulated Raman and stimulated Brillouin scattering involve the excitation of optical and acoustic phonons, respectively. Stimulated Raman scattering (SRS) is a relatively broadband, though not instantaneous process and typically involves frequency shifts of terahertz (THz) or greater due to the absorption or emission of the phonon. Because one can design a fiber laser cavity to limit the bandwidth of optical components that are subject to strong feedback to 100 gigahertz (GHz) using commercially available components, SRS can be ignored with a proper choice of laser cavity. Stimulated Brillouin scattering (SBS) typically involves frequency shifts on the order of 10 GHz and has the highest gain of nonlinear processes observed in optical fibers with a gain coefficient on the order of 50 $W^{-1}km^{-1}$ in the 1.55-μm spectral region [7]. However, SBS is a narrowband process due to the finite lifetime of the acoustic phonon with a resonant bandwidth on the order of 10 MHz. Finally, in the section of the fiber that is doped with the gain medium, changes in the refractive index and gain will occur due to saturation and thermal effects associated with the pumping and, possibly, the establishment of inhomogeneous distributions of the resonant species due to spectral and spatial hole burning. If

the nonlinear contributions are small, then the resonant transition can be modeled similarly to the nonresonant background, with appropriate changes in the gain and index coefficients.

In addition to these nonlinear processes, the fiber has a linear dispersive characteristic that leads to group velocity dispersion. This is important for broadband, short pulse propagation. However, one can spectrally limit the feedback bandwidth in the lasers. Therefore, if we ignore stimulated Raman scattering and group velocity dispersion. The coupled equations for the complex amplitudes of the forward, A_f, and backward, A_b, waves within a linear fiber laser cavity, and the associated time-dependent equation for the Brillouin interaction, then become [8]:

$$\pm\frac{\partial A_{f,b}}{\partial z}+\frac{1}{v_g}\frac{\partial A_{f,b}}{\partial t}-\frac{\alpha}{2}A_{f,b}=(-\beta+i\gamma)\left(\left|A_{f,b}\right|^2+2\left|A_{b,f}\right|^2\right)\mp\frac{g_b}{2}A_{b,f}Q \qquad (1)$$

$$T_B\frac{\partial Q}{\partial t}+(1+i\,\delta)Q=A_{f,b}A_{b,f}^* \qquad (2)$$

Here, z is the spatial coordinate, v_g is the group velocity, α is the linear gain or loss term, β and γ are the gain saturation and self-phase modulation coefficients, respectively. The terms g_B, T_B and Q relate to Brillouin scattering in the fiber. In the equation for the backward propagating wave, Q, which is related to the density oscillations that accompany acoustic waves in the medium, is replaced by Q^*. The detuning parameter δ is defined as $\delta=(\omega_f-\omega_b-\Omega_B)T_B$ where $\omega_{f,b}$ is the instantaneous frequency of the respective waves, Ω_B is the frequency of the acoustic wave, and T_B is the lifetime or inverse decay rate of the acoustic wave. Determining how the coefficients in Equations 1 and 2 can be used and manipulated to produce self-control of the cavity phase, and self-organization of an array of intracavity coupled lasers could be a fruitful area for further research.

REFERENCES

[1] V. Dominic, S. MacCormack, R. Waarts, S. Sanders, S. Bicknese, R. Dohle, E. Wolak, and E. Zucker, "110 W Fiber Laser," *Proceedings Conf. Lasers and Electro-Optics (CLEO) '99*, Baltimore, MD 1999, Postdeadline Paper CPD11-1.

[2] D.C. Brown and H.J Hoffman, "Thermal, Stress and Thermo-Optic Effects in High Average Power Double-Clad Silica Fiber Lasers," *IEEE J. Quantum Electron.* **37**, 207 (2001).

[3] Y. Kono, M. Takeoka, K. Uto, A. Uchida, and F. Kannari, "A Coherent All-Solid-State Laser Array Using the Talbot Effect in a Three-Mirror Cavity," *IEEE Journal of Quantum Electronics* **36**, 607 (2000).

[4] V.A. Kozlov, J. Hernandez-Cordero, and T.F. Morse, "All-fiber Coherent Beam Combining of Fiber Lasers," *Opt. Lett.* **24**, 1814 (1999).

[5] Bartelt-Berger, U. Brauch, A. Giesen, H. Huegel, and H. Opower, "Power-Scalable System of Phase-Locked Single-Mode Diode Lasers," *Ap. Opt.* **38**, 5752 (1999).

[6] G.P. Agrawal, *Nonlinear Fiber Optics, 3rd Edition*, Academic Press, 2001.

[7] A.R. Chraplyvy, "Limitations on Lightwave Communications Imposed by Optical-Fiber Nonlinearities," *J. Lightwave Technol.* **8**. 1548 (1990).

[8] D. Yu, W. Lu, and R.G. Harrison, "Physical Origin of Dynamical Brillouin Scattering in Optical Fibers With Feedback," *Phys. Rev. A.* **51**, 669 (1995).

DISTRIBUTION LIST

DTIC/OCP 8725 John J. Kingman Rd, Suite 0944 Ft Belvoir, VA 22060-6218	1 cy
AFRL/VSIL Kirtland AFB, NM 87117-5776	2 cys
AFRL/VSIH Kirtland AFB, NM 87117-5776	1 cy
Jaycor, Inc 3394 Carmel Mountain Road San Diego, CA 92121	1cy
Official Record Copy AFRL/DELO/Dr. Phillip Peterson	2cy